Geomorphology 318 (2018) 404–420

Contents lists available at ScienceDirect

Geomorphology

journal homepage: www.elsevier.com/locate/geomorph

Impacts of gravel mining and renaturation measures on the sediment flux and budget in an alpine catchment (Johnsbach Valley, Austria)

Eric Rascher [a,*], Rolf Rindler [b], Helmut Habersack [b], Oliver Sass [a]

[a] University of Graz, Department of Geography and Regional Science, Heinrichstrasse 36, 8010 Graz, Austria
[b] University of Natural Resources and Life Sciences, Institute of Water Management, Hydrology and Hydraulic Engineering, Muthgasse 107, 1190 Vienna, Austria

ARTICLE INFO

Article history:
Received 26 February 2018
Received in revised form 9 July 2018
Accepted 10 July 2018
Available online 11 July 2018

Keywords:
Sediment budget
Gravel mining
DEM of difference
Integrative bedload monitoring

ABSTRACT

In the Johnsbach Valley (Austria), a medium size non-glaciated torrent catchment, enormous amounts of sediment have been made available due to the brittle dolomite bedrock. This occurs mainly in the Zwischenmäuerstrecke (ZMS) (English translation: "reach between the walls") and presents a major challenge to local river management. Within a renaturation project, which followed several decades of disturbance (flood protection and gravel mining) in the ZMS, it is of particular importance to understand where the sediments come from and the transport pathways through the system to prepare future forecasts.

In the present study, we investigate the recent sediment cascade in a comprehensive analysis of the ZMS that was achieved by means of airborne laser scanning campaigns in 2010 and 2015. The current bedload yield at the outlet was measured using an integrative bedload monitoring system. Historical data from 1954 was used to illustrate the effects of the mining period on the former sediment routing. Finally, we evaluated the expected sediment transport rates in the near future.

The results show that from the hillslopes sediments are mainly transported via the active side trenches to the main channel (~7000 $m^3\ yr^{-1}$). The sediment transport in the Johnsbach River consists mainly in relocating the periodically occurring sediment entries of the side trenches. The bedload transport rates at the outlet sum up to annual bedload yields of 2000 $m^3\ yr^{-1}$ to almost 12,000 $m^3\ yr^{-1}$ during the observation period. Especially those areas inside the side trenches that were heavily affected by gravel mining (excavated amount of sediment during the mining period: ~25,000 $m^3\ yr^{-1}$) are now accumulating sediment since the end of this period (~8000 $m^3\ yr^{-1}$). Future scenarios will depend heavily on the progress in the mining affected side channels. The impacts of this period are continuously being reworked and a natural sediment flow will adjust in the near future. The sediment input into the Johnsbach River will rise significantly and could lead to a doubling in the annual sediment yield at the outlet compared to now. In particular, the reaches along the Johnsbach River following the confluences with the mining affected side trenches are already showing morphological changes due to the recently imported sediments.

1. Introduction

Over the last decades alluvial rivers, all over the world and especially in Europe, have been significantly affected by human disturbances (Petts, 1989). The most common forms of intervention in fluvial systems are due to land-use changes, urbanization, dams and reservoirs constructed to generate hydroelectric power, flow diversions, and gravel and sand mining. Several studies (e.g., Marston et al., 1995; Bravard et al., 1997; Liébault and Piégay, 2001, 2002; Surian and Rinaldi, 2003; Liébault et al., 2005; Rinaldi et al., 2005; Rivora et al., 2005; Spink et al., 2009; Surian et al., 2009a, 2009b) have shown that these disturbances cause remarkable channel changes with substantial effects on flow and sediment regimes. Induced by a loss of sediment supply and recharge, a range of environmental and social effects result from channel incision and narrowing, such as undermining of structures, loss of groundwater storage or loss of habitat diversity (Bravard et al., 1999). Especially in the Alps, this has led to the fact that only a minor portion of all rivers are still in a natural or near-natural condition (Martinet and Dubost, 1992; Ward et al., 1999). To overcome this problem, a need for sustainable sediment management arises by defining river restoration strategies (Piégay et al., 2005; Habersack and Piégay, 2008; Liébault et al., 2008; Rinaldi et al., 2009).

From historical times alluvial rivers have been attractive sources for sediment exploitation. Notably, 'in-stream mining', which involves the removal of sediment from the river bed, directly affects the channel geometry resulting in an imbalance of sediment supply and transport capacity (Sandecki, 1989). By changing the geomorphic setting many

* Corresponding author.
E-mail address: eric.rascher@uni-graz.at (E. Rascher).

https://doi.org/10.1016/j.geomorph.2018.07.009

different environmental and economic impacts can be expected (Bravard et al., 1999), which are summarized by Rinaldi et al. (2005) and Rivora et al. (2005). Throughout the literature it has been widely discussed what consequences can arise from mining the active river channel. Certainly it is not only the actions involving the river itself that cause a disturbed sediment management but also interventions (mining gravel in pits) affecting the contributing side channels and catchments that are connected to specific river reaches.

Several different human disturbances have heavily affected the alluvial channel in the Johnsbach catchment since the middle of the past century. These include works for flood and bank protection, gravel mining in sediment suppling side catchments to the main river system, and in recent years river restoration that includes an explicit sediment management. After a major flood event in 1949, which destroyed the only access into the Johnsbach Valley, the course of the river was armed with longitudinal barriers and check dams along the ZMS between 1950 and 1974 (Thonhauser, 2007; Kammerer, 2008). The goal was to compress the course of the river and to force the stream into a man-made river bed (Haseke, 2006). Former gravel mining in two of the biggest side catchments (in Gseng and Langgries since 1984 and 1991, respectively) was interrupting the sediment flux in those channels as huge amounts of sediment were excavated and used industrially. The annual amount of sediment being removed from those side catchments is reported to be 15,000–20,000 $m^3\ yr^{-1}$ (Haseke, 2011). With the establishment of the National Park (NP) Gesäuse in 2002, the excavation of sediment had to be abandoned but was not terminated before 2008 because of still ongoing contracts. Finally, both former mining areas were restored from 2009 to 2010. Meanwhile, the Johnsbach River was renaturated in the cost-intensive European Union funded river-ecological LIFE-project “Conservation strategies for woodland and wild waters in the Gesäuse” controlled by the NP Gesäuse from 2006 to 2009. The main focus of this project was to dismantle and widely remove extensive engineering measures in the river and at the junctions to the side channels (Haseke, 2011). This was meant to ensure that sediment can reach the Johnsbach River and finally the River Enns in sufficient quantities according to its natural dynamics (Holzinger et al., 2012). During the LIFE-project the new concept involved several interventions: adjusting the slope of the river and avoiding high steps effectuated by building broad, but flat ground sills, expanding the obstructed banks and releasing the Johnsbach River between the sills (Haseke, 2011). In this way the Johnsbach River is now able to rebuild its original gravel banks and furcations, ballasts the new sills and therefore creates valuable habitats and ensures fish migration. Furthermore, an increase in coarse material prevents the progress of river-bed sealing through fine-grained material during the last decades and thus prevents groundwater subsidence as well as the reduction of micro habitats (Holzinger et al., 2012).

Fischlschweiger (2004) investigated the aftermath of the mining activities in the lower Langgries side catchment, concluding that 10,000 $m^3\ yr^{-1}$ needed to be excavated (in the reference period of 1993–2002) to maintain the current state. Several authors (Kammerer, 2006a, 2006b; Zulka, 2013) were focusing on changes in the evolution of habitats due to mining and its resulting effects. They all could prove that mining activities disrupt the fragile balancing system of scree slopes, which in turn affects the habitats of certain fauna and flora. In 2013, the FWF-funded Sedyn-X project was launched to investigate sediment transport in the ensuing field of tension between nature conservation (e.g., aqua fauna habitats), hazard protection and the efficiency of hydropower stations downstream. By now, Stangl et al. (2016) have applied a sediment connectivity analysis combining upslope contributing area and downslope flow length. According to their analysis, sediment storages close to the main river are highly coupled to the outlet, whereas erodible sediments in the remote high-alpine areas are not. Rascher and Sass (2017) quantified surface changes using multi-temporal terrestrial laser scanning at the interface between the main torrent and selected tributary channels. They could show that the sediment output of tributaries is currently limited (seasonal and event based) as sediment is “missing” due to the mining history. The objective of this study is to set up a sediment budget, enabling the analysis of the impacts of gravel mining and renaturation on the sediment flux in the ZMS of the Johnsbach Valley. To this end, we investigated the recent sediment cascade focusing on several aspects. First, how much sediment is provided from rock walls to the side-catchments (quantifying the input parameter for the sediment budget). Second, where and to which extent is sediment relocation currently taking place (evaluating transport and storage in the system). Third, how much sediment is exported out of the Johnsbach Valley (quantifying and comparing the fluvial sediment transport to the sediment output). Fourth, we show the effects of the mining period on the former sediment routing by reconstructing the sediment cascade in the relevant areas. Finally, we predict the sediment transport rates in the near future once decoupled side catchments are reconnected to evaluate the overall consequences of the recent renaturation measures. Coupled investigations of sediment cascades and bedload transport have rarely been carried out. Therefore, our approach could be a showcase example describing the spatial sediment dynamics on the one hand and verifying the predicted sediment yield on the other hand, in an area that underwent significant anthropogenic modifications in the past.

2. Regional-scale setting and local-scale classification of the study site

2.1. Characterization of the study area

The Johnsbach Valley (Fig. 1) is a non-glaciated alpine catchment in Upper Styria (Austria) that covers an area of approximately 65 km^2 reaching from 584 m a.s.l. at the outlet to 2369 m a.s.l. (Hochtor). The valley is drained by the Johnsbach River, which runs for 14 km with a mean gradient of almost 4% before it empties into the River Enns. The geological setting is characterized by different rock types belonging to two nappes, the Northern Calcareous Alps in the north and the Greywacke Zone in the south (e.g., Ampferer, 1935; Hiessleitner, 1935; Flügel and Neubauer, 1984). Our area of investigation, the Zwischenmäuerstrecke (ZMS), is situated in Triassic carbonate rocks, mainly limestone (Dachsteinkalk) and dolomite (Wettersteindolomit) (Figs. 2B and 3A). The ZMS is a 4.5 km river reach with a catchment of around 13 km^2 in size that is sparsely vegetated (Fig. 3C) by fir forests and pine shrub lands, and is shaped by steep furrows and deeply incised channels (Fig. 3B) on both sides. The majority of the sediment that is relocated and transported in the Johnsbach Valley is stored in the ZMS.

The climate is characterized by annual mean temperatures of around 8 °C in the lower elevations of the valley and below 0 °C in the summit regions. Annual precipitation amounts to approximately 1500–1800 mm (Wakonigg, 2012a, 2012b). Storm precipitation occurs almost exclusively in the summer months and can reach several tens of mm per hour. Thus, runoff at the Johnsbach River peaks in spring (snow melt) and summer while the tributaries show surface runoff and sediment transport only during episodic rainstorms.

The combination of the geological setting and the climatic conditions results in high morphodynamic activity, primarily in the ZMS (Strasser et al., 2013). The brittle Wetterstein Dolomite is particularly prone to weathering, providing large amounts of sharp-edged debris. This debris is being reworked and relocated by rock falls and debris avalanches from the rock walls over the steep slopes into the channels of the side catchments. Finally, this results in high sediment input rates into the Johnsbach River (Rascher and Sass, 2017).

2.2. ZMS – Subdivision of river sections and side catchments

Following Lieb and Premm (2008), the ZMS can be divided into three segments (Figs. 2B and 3D) according to its landscape and its morphodynamics. The southern section (III) is dominated by a very steep landscape (with mean slope angles of >50°) and characteristic

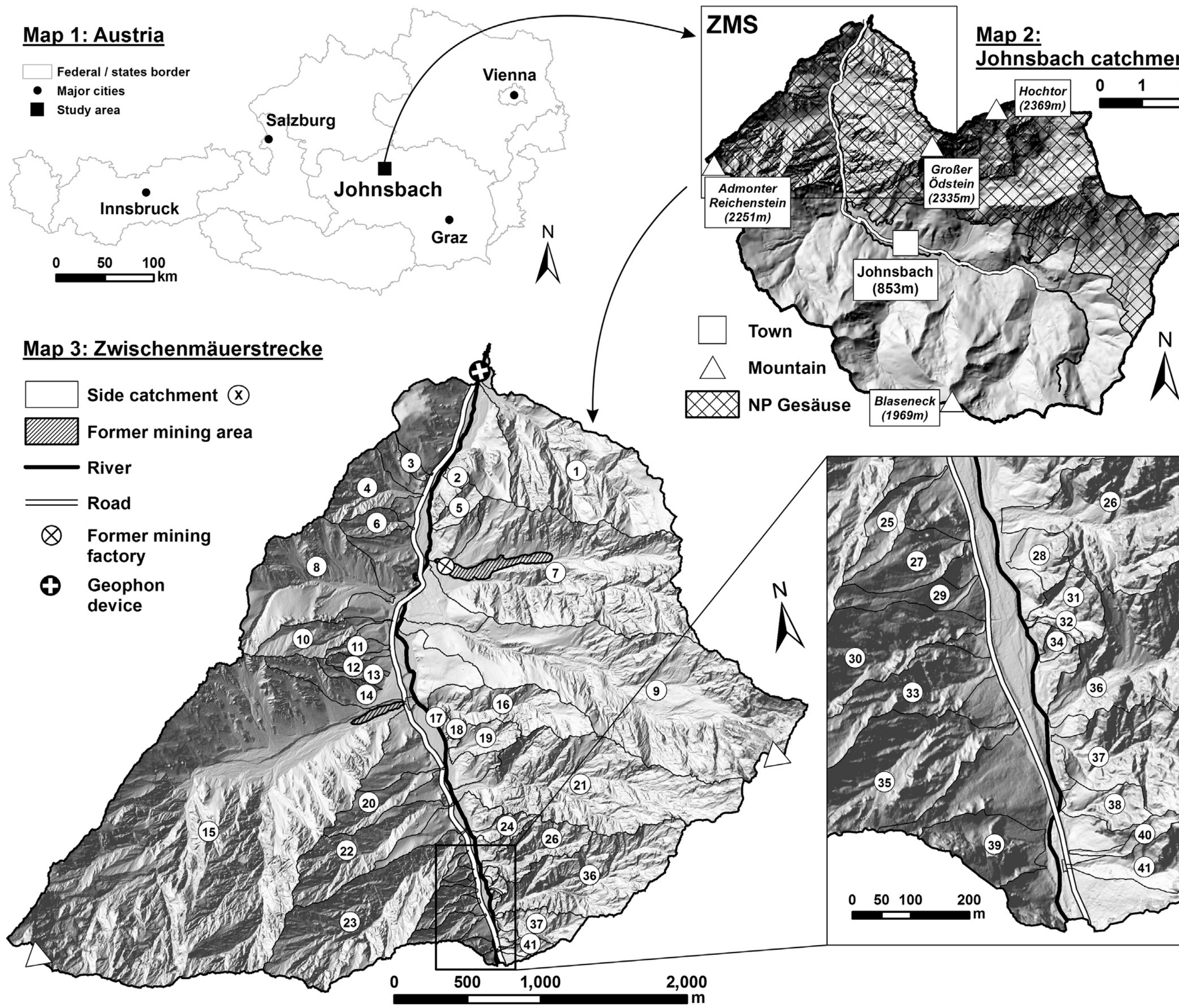

Fig. 1. Location of the study area (with inset map of Austria and the catchment), hillshade map of a LiDAR-derived DEM (2015, © Bureau of the Styrian Government). The numbers in map 3 correspond to the side catchments, listed in Table A.2.

erosional patterns formed into the dolomite bedrock (Fig. 3A). It covers the side catchments ranging from the Silberreith Bridge down to Langgries side catchment at a 2 km river reach. The central area (II) is shaped more smoothly as the dolomite bedrock is largely covered by breccia that prevents the carbonate bedrock from being eroded. In this 1.5 km river reach the biggest side catchments in the ZMS (Langgries, Kainzenalbl, Koderalbschütt and Gseng) run into the Johnsbach River in which most of the sediment is being transported. In the lowest section (I), until the Johnsbach River meets the River Enns, the valley gets narrow again with limestone being the dominant bedrock type. Shortly downstream, a 500 m long alluvial plain is the last sediment storage. For the purpose of our study all three river segments were divided into two reaches (A and B) of similar morphological structure (Fig. 3, Table A.1).

Several side catchments discharge into each river segment from both sides (Fig. 3D). Forty one side catchments (Table A.2) were identified through field campaigns in combination with ArcGIS routines. The ZMS was mapped by Krenn (2016) (Fig. 3B) with emphasis on geomorphic processes and storage types. The spatial bedrock distribution, the slope catchments (SL) (total of 131) and channel sections (CH) (total of 99) were outlined in each of the side catchments. Along the Johnsbach River, six alluvial sections (AS) where defined following the classification into the river segments and reaches.

3. Methodological framework

3.1. Reconstructing the sediment cascade

To evaluate the sediment output of the ZMS, the sediment cascade was assembled (Fig. 4 right). Side catchments (e.g., A in Fig. 4) inside the ZMS were outlined in which slope catchments (e.g., SL_{A1} in Fig. 4), each including its spatial bedrock extent (e.g., $wRWI_{A1}$ in Fig. 4), and channel sections (e.g., CH_{A1} in Fig. 4) were separated. At each side catchment sediment volumes were propagated through the system from the SL to the CH and along the CHs down to the respective alluvial section (e.g., AS_I in Fig. 4). Several side catchments can contribute to each AS. The same is valid for the fluvial system, where sediment input occurs from the side catchments at certain AS and is then routed downstream. Sediment propagation (according to the rules defined in Fig. 4, bottom right) was determined as follows:

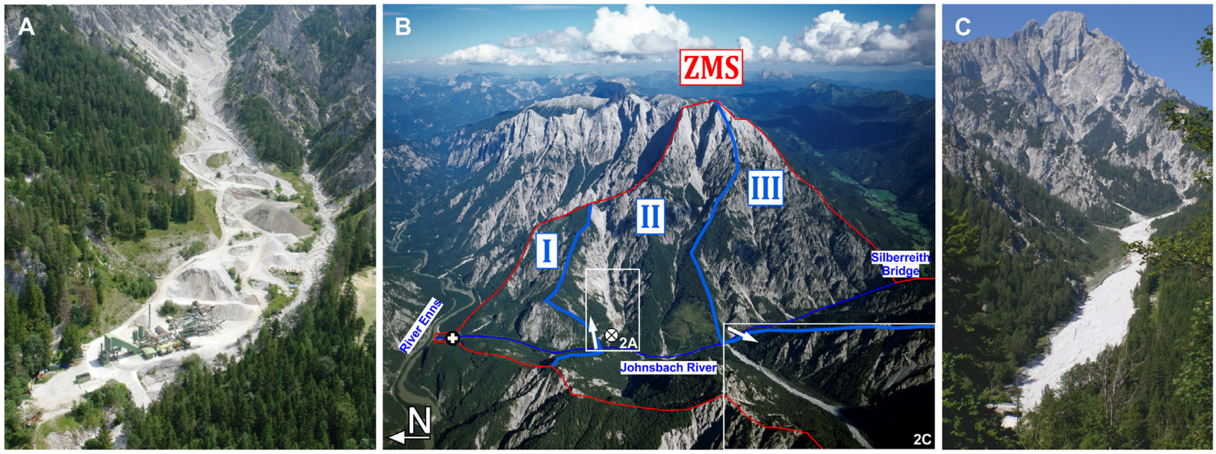

Fig. 2. Photographs from the Johnsbach Valley: (A) Gseng side catchment in eastward direction with the former mining factory in the front (picture by NP Gesäuse, 07/2006); (B) aerial image (eastward direction) of the ZMS (red outline) with I–III indicating the three river segments; white rectangles and arrows indicate the location and direction of sight of pictures 2A and 2C, respectively; point features (location of the bedload monitoring system and the former mining factory) correspond to Fig. 1 (picture by NP Gesäuse, 10/2004); (C) Langgries side catchment (07/2013) in westward direction with the road bridge in the front and the Admonter Reichenstein in the back.

if net erosion occurs in a specific SL, CH, or AS, this volume is transported farther down (to the next CH, AS, and so on), if net deposition occurs there is no further transport. Accordingly, the net storage value of a specific CH or AS can change due to the impact of an adjacent SL, CH or AS.

3.2. Data acquisition

3.2.1. Light detection and ranging (LiDAR) data

The LiDAR data used to derive the Digital Elevation Models (DEM) for 2010 (company *AVT*) and 2015 (company *Vermessung Schmid*)

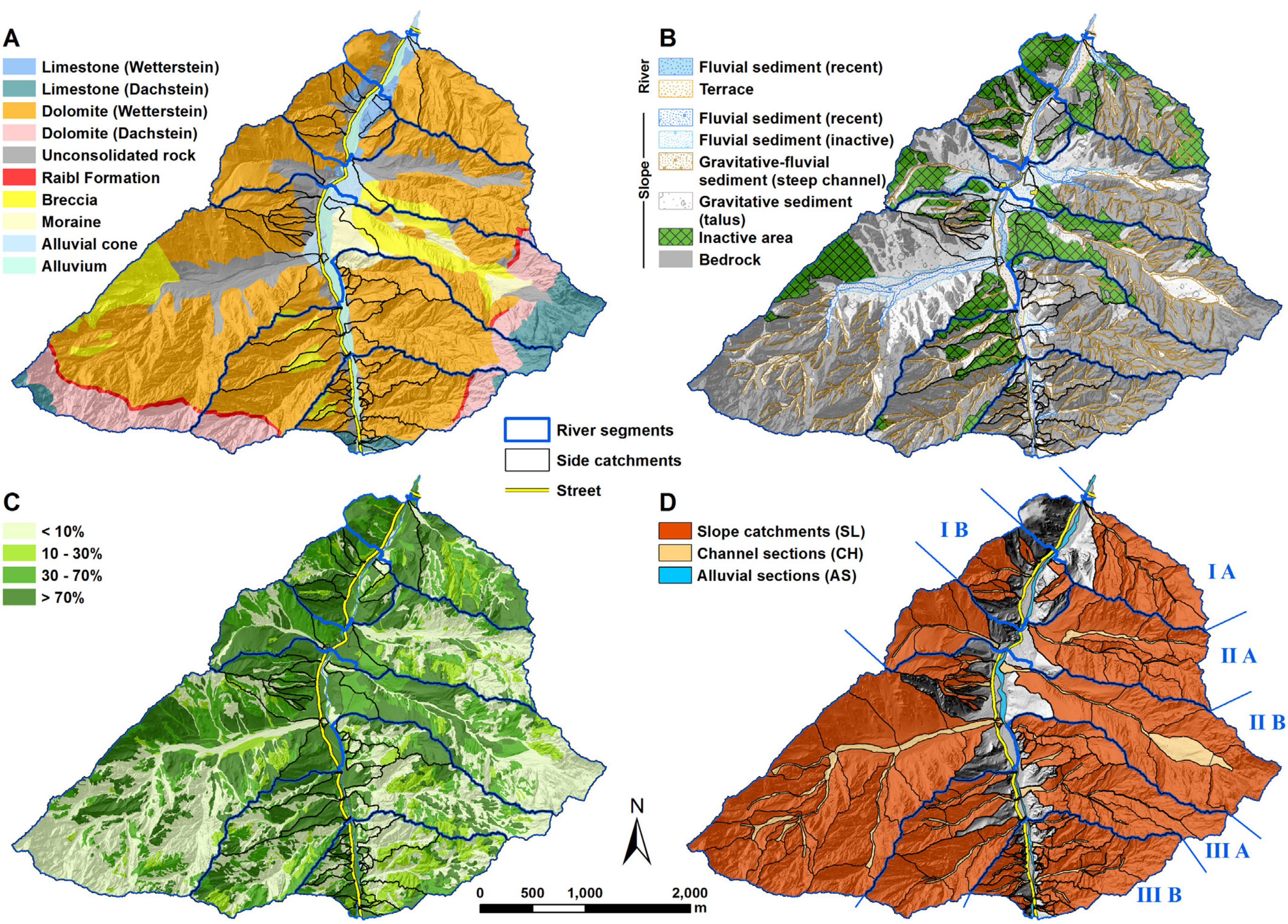

Fig. 3. Characteristic maps of the ZMS: (A) geology (modified from Ampferer, 1935); (B) geomorphology/sediment storage types (modified from Krenn, 2016); (C) vegetation cover (derived from HAPITALP mapping by NP Gesäuse); (D) subdivision (as defined in Section 2.2), I A to III B are the three segments and their sub-reaches; hillshade map of a LiDAR derived DEM (2015, © Bureau of the Styrian Government).

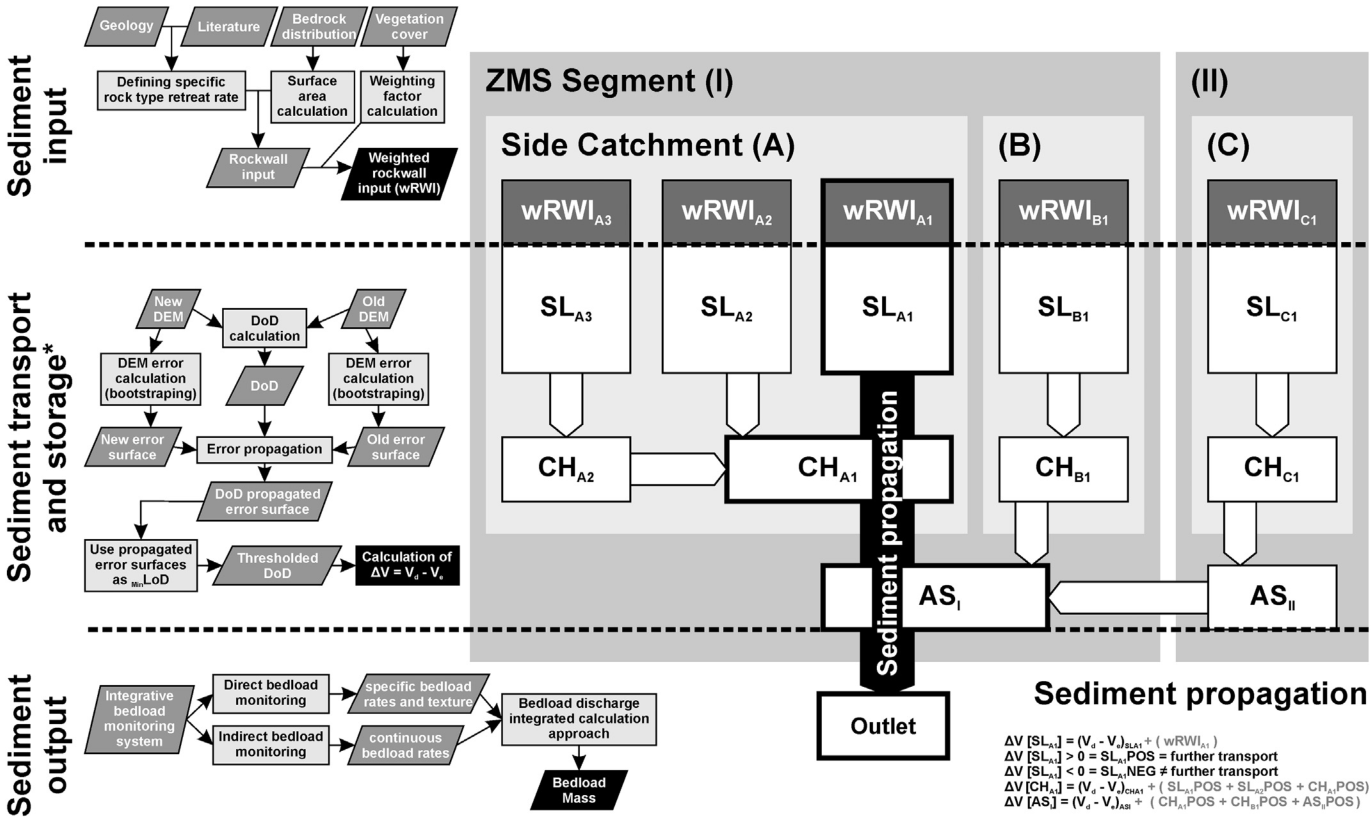

Fig. 4. Flow chart of the reconstructed sediment cascade and workflows for determining change detection at each stage in the sediment budget. Note: Erosion (V_e) and deposition (V_d) estimates, weighted rockwall input (wRWI), slope catchment (SL), channel section (CH), alluvial section (AS); *: simplified from Vericat et al., 2017.

were recorded via Airborne Laser Scanning (ALS). The flights were carried out using two scanning systems (Riegl LMS-Q560/Q680) mounted on a Eurocopter AS350 with a desired minimum survey design point density of 4 pts m^{-2}. In 2015 the Karl-Franzens-University contracted a second LiDAR survey of the Johnsbach Valley. The survey was carried out on 26 August 2015 using a Riegl LMS-Q780 mounted on a Piper PA34 with a desired minimum survey design point density of 4 pts m^{-2} as well. Both raw point clouds were filtered into ground/non-ground points using *TerraScan* software classification routines and algorithms and finally clipped to the ZMS. The filtered point density was 7.35 and 5.50 pts m^{-2} for 2010 and 2015, respectively. Bare ground points were then triangulated into temporary Triangular Irregular Networks and finally rasterized to derive DEMs with a homogeneous resolution of 1 m using the *LAStools* software algorithms.

3.2.2. Historic areal data

To quantify the loss of sediment since the beginning of gravel mining in the side catchments Gseng and Langgries, 5 m DEMs were created by the company *AVT* using the areal images from 1954. For this purpose 3D ground control points were derived from an existing survey and later used in *Match-AT* for the orientation of the 1954 areal images. The following stereoscopic analysis for deriving height information was accomplished using *Summit Evolution*. The DEMs cover the channels of both side catchments where the mining took place and the adjacent areas that are directly affected.

3.2.3. Additional input variables

Additional input parameters, which are mostly provided by Krenn (2016), were necessary. The geological map of the study area (Fig. 3A) was newly digitized and modified after Ampferer (1935). A map on the vegetation cover (Fig. 3C) was provided using the results of the HABITALP (Alpine Habitat Diversity) mapping carried out by the NP Gesäuse. A geomorphological map showing the dominant features and storage types was developed by Krenn (2016). Mapped bedrock areas were compared to the geological map to assess the type of rock present.

3.2.4. Integrative bedload monitoring system

An integrative monitoring system like at other sites in Austria is installed at the Johnsbach River (for location see Figs. 1 and 2B) that combines direct and indirect monitoring devices (Rickenmann et al., 2014; Habersack et al., 2017; Rickenmann and Fritschi, 2017). It is not possible to monitor bedload transport processes satisfactorily using only a single measurement device, as each method has its specific advantages and restrictions (Kreisler et al., 2017). Hence, the integrative bedload monitoring system was developed to overcome this challenge. It consists of a basket sampler, bedload traps and geophone devices (see arrangement in Fig. 5). As the deficits can be compensated by combining the different direct and indirect methods, the monitoring system offers the possibility to comprehensively monitor bedload transport processes.

Direct bedload monitoring methods enable the determination of (specific) bedload rates and the texture of the bedload material. In the following, the basket sampler and the bedload trap, both part of the integrative monitoring system at the Johnsbach River, are introduced. Mobile basket samplers have been applied in bedload monitoring for decades (Mühlhofer, 1933; Van Rijn, 1986). At the Johnsbach River an adapted type of the Bunte sampler with an intake width of 0.5 m and a net with 2–4 mm pore size is deployed (Bunte et al., 2004; Kreisler et al., 2017). Using a mobile crane, the sampler is lowered from the riverbank onto the riverbed. Measurements are conducted at defined verticals directly upstream from the geophone device and the position of the basket sampler is fixed with two tether lines (Kreisler et al., 2017). The measuring time depends on the prevailing bedload transport rate.

At the bedload traps the sample box is covered by a lid with a longitudinal sampling slot. The sampling slots are 1.6 m long and 0.5 m

Fig. 5. Arrangement of the integrative bedload monitoring system consisting of a bedload trap and a geophone bar (center and lower right) supported by a basket sampler (upper right). Bedload data acquisition and river gauging takes place in a monitoring station (left). Note: views in the center and the upper right are looking upstream.

wide. Upon start of the monitoring, the slot is opened hydraulically via manual control, the transported bed material gets trapped in the sample box and load cells automatically record the mass increase within the box. Bedload traps enable measurements at all discharge stages and thereby also the bedload can be monitored even during flood events (Habersack et al., 2017; Kreisler et al., 2017). Habersack et al. (2017) showed that both hydraulic and sampling efficiency is high. Furthermore, the simultaneous measurement of bedload rates and the determination of bedload texture is possible. Disadvantages of the bedload trap are its fixed position in the stream bed and the high maintenance efforts required.

Geophones are vibration sensors originating from seismic technology. To detect bedload transport, the geophone sensors are mounted on the bottom side of 0.36 m long, 0.5 m wide and 0.015 m thick steel plates (Habersack et al., 2017). These steel plates are embedded in the stream bed. Bedload particles moving over the steel plates produce vibrations which are registered by the geophone sensors. The geophone signal is sampled continuously at a rate of 10 kHz. Geophone data and bedload mass correlate well when the bedload material is larger than 10–30 mm (Rickenmann and McArdell, 2007; Wyss et al., 2016).

3.3. Data processing

3.3.1. Rock wall retreat as sediment input

Sediment input into the system derives from the rock walls surrounding the ZMS. As only fragmentary measurements of rock wall retreat rates are available in the study area, rates from other investigations (Sass and Wollny, 2001; Glade, 2005; Sass, 2005, 2007; Vehling, 2016) working in similar settings or rock types were used. This is a very simplified approach not taking into account spatial variability due to, for example, singular events, joint density or dip of strata. The real bedrock surface area was calculated and combined with retreat rates of 1.0 mm yr^{-1} and 0.3 mm yr^{-1} for dolomite and limestone dominated rock types, respectively. Finally, the input values were weighted using the vegetation cover as a proxy for erosivity in a reverse proportional manner (100% vegetation cover = 0% erosivity, and vice versa), which is a simplifying assumption (Fig. 4, top left).

3.3.2. DEM of difference (DoD) and volume calculation

Because the morphology of our study area is complex and the available DEMs are heterogeneous in their quality and accuracy, the assessment of erosion and deposition volumes needs a robust approach to discriminate between actual surface elevation changes and the inherent noise. We therefore consider DoD uncertainties by following the three main steps proposed by Wheaton et al. (2010): (1) estimating the magnitude of individual DEM uncertainty in a spatially variable way using a bootstrapping approach; (2) propagating the identified uncertainties into the DoD, and (3) assessing the significance of the propagated uncertainty (Fig. 4, middle left).

The spatially variable uncertainty assessment was performed by applying a bootstrapping experiment, which is basically a statistical resampling technique. The principle is that a sub-sample is removed from the sufficiently large data set and the DEM is reconstructed without it (Wheaton, 2008). The removed sub-sample is then used to estimate the elevation uncertainty through comparison. In our study, a random sample of 10% of the points was removed from the original data set. The thinned data set was then triangulated and converted into a 1 m DEM (for 2010 and 2015) and a 5 m DEM (for 1954), respectively. The elevations of the sub-sample points (Z_{xy}) were compared to the DEM values (Z_{DEM}) such that the mean difference ($\overline{|Z_{xy} - Z_{DEM}|}$) is an indication of elevation uncertainty. This was repeated with three different random sub-samples to ensure consistency in the results (Table 1). Finally, point clouds representing the areas of interest (AS, SL and CH) were separated from the original ALS data set. Using the elevation uncertainty information (Table 2) in the sub-samples, 1 m error surfaces were created (via triangulation).

Assuming a normal distribution of errors, we follow the existing approaches for propagating uncertainties into DoDs (Taylor, 1997; Brasington et al., 2003; Fuller et al., 2003; Lane et al., 2003) according to the equation:

$$U_{crit} = t\left(\sqrt{(\delta z_{new})^2 + (\delta z_{old})^2}\right) \quad (1)$$

where U_{crit} is the critical threshold in the DoD (or the minimum level of detection (LoD) threshold) and δz_{new} and δz_{old} are, respectively, the

Table 1
Point survey and sampling statistics for bootstrapping approach. (GS = Gseng, LA = Langgries, SL = slope catchments, CH = channel sections, AS = alluvial sections).

		1954 (GS)	in %	1954 (LA)	in %	2010 (ZMS)	in %	2015 (ZMS)	in %
Original	Total	13,832	100.00	12,640	100.00	140,841,374	100.00	72,626,846	100.00
Sub sample 1	Total	1389	10.04	1261	9.98	13,744,287	9.76	7,316,341	10.07
	SL	1201	8.68	744	5.89	4,174,705	2.96	2,227,759	3.07
	CH	189	1.37	516	4.08	737,478	0.52	398,144	0.55
	AS	n.a.	n.a.	n.a.	n.a.	89,021	0.06	58,429	0.08
Sub sample 2	Total	1388	10.03	1263	9.99	13,744,287	9.76	7,316,341	10.07
	SL	1199	8.67	783	6.19	4,174,407	2.96	2,228,222	3.07
	CH	190	1.37	479	3.79	737,681	0.52	398,211	0.55
	AS	n.a.	n.a.	n.a.	n.a.	88,990	0.06	58,464	0.08
Sub sample 3	Total	1373	9.93	1263	9.99	13,744,287	9.70	7,316,341	10.07
	SL	1184	8.56	775	6.13	4,174,583	2.96	2,228,362	3.00
	CH	188	1.36	488	3.86	737,662	0.52	398,234	0.55
	AS	n.a.	n.a.	n.a.	n.a.	88,950	0.06	58,480	0.08

elevation uncertainty in the newer and the older DEM. U_{crit} is based on a critical Student's t-value at a chosen confidence interval:

$$t = \frac{|Z_{DEM_{new}} - Z_{DEM_{old}}|}{\delta u_{DoD}} \tag{2}$$

where δu_{DoD} is the propagated error in the DoD and $|Z_{DEM_{new}} - Z_{DEM_{old}}|$ is the absolute value of the DoD. The 95% confidence interval was used as a threshold throughout this paper. For each DoD raster cell, a critical threshold error was then calculated with Eq. (1) to derive a LoD that was finally subtracted from all DoD cells to derive maps of significant elevation change and calculate volumes of erosion and deposition (by multiplying with the appropriate raster cell size value). The final DoD maps were derived according to the above mentioned methodology using the GCD (Geomorphic Change Detection) v6.1.6 software ArcGIS plugin developed by Wheaton et al. (2010).

3.3.3. Calculating the total bedload mass

The amount of bedload mass V_b at the Johnsbach River was calculated using the Bedload Discharge Integrated Calculation Approach (Habersack et al., 2017). Direct measurement devices were used to determine the bedload discharge q_b (kg m^{-1} s^{-1}). By combining geophone data from a plate located directly downstream of the direct measurement devices, geophone calibration could be undertaken (Fig. 4, bottom left). Using the geophone information of the spatial distribution, the cross-sectional bedload discharge Q_b (kg s^{-1}) could be calculated by integrating the specific bedload discharges q_b over the stream width w_{cs}:

$$Q_b = \int_{w_{cs}=1}^{w_{cs}=n} q_b \, dw_{cs} \tag{3}$$

To determine the total bedload mass V_b, the cross-sectional bedload discharge Q_b was integrated over a specified time period t:

$$V_b = \int_{t=1}^{t=n} Q_b \, dt \tag{4}$$

4. Results

4.1. Rock wall retreat as sediment input

Sediment input from rock walls was calculated by applying published rock wall retreat rates to the geological setting and the particular types of rock (Fig. 3A). Volumetric sediment input values were calculated for each slope catchment downslope of rock walls (Fig. 6). The annual input rates vary between 0 and 340 m^3 yr^{-1} depending on the type of rock, the relevant retreat rate, and the areal amount of bedrock in the slope catchment. High amounts of sediment input correspond with the higher retreat rates of the widespread dolomite bedrock (Fig. 3A). Nevertheless, the highest rates were calculated for the Dachstein Limestone areas at higher altitudes (in the SE and SW of ZMS) with steep slopes and therefore large bedrock areas.

4.2. DEMs of difference (DoDs)

DoDs (Figs. 7 to 9) for the ZMS (2010–2015, 1 m raster cell size) and for two main side channels (1954–2010, 5 m raster cell size) show the spatial patterns of geomorphic change in the ZMS and the effects of the gravel mining during the period 1954–2010. In the following, the two time periods before (Figs. 7A and 8A) and after 2010 (Figs. 7B, 8B and 9) are presented separately.

4.2.1. Historic (1954–2010)

At Gseng, mainly erosion (debris removal) prevails especially in the area of former gravel mining (Fig. 7A). Elevation differences in the

Table 2
Summary of elevation uncertainty [m] statistics. (GS = Gseng, LA = Langgries, SL = slope catchments, CH = channel sections, AS = alluvial sections).

		1954 (GS)		1954 (LA)		2010 (ZMS)			2015 (ZMS)		
		CH	SL	CH	SL	AS	CH	SL	AS	CH	SL
Sub sample 1	Min	0.01	0.00	0.01	0.01	0.00	0.00	0.00	0.00	0.00	0.00
	Max	3.82	16.29	13.76	6.49	7.34	51.40	73.16	6.35	50.53	68.17
	Mean	0.48	0.94	0.52	0.70	0.13	0.43	0.49	0.12	0.44	0.50
	Std.-dev.	0.52	0.91	0.85	0.80	0.20	0.81	0.73	0.18	0.87	0.76
Sub sample 2	Min	0.01	0.01	0.01	0.02	0.00	0.00	0.00	0.00	0.00	0.00
	Max	5.44	15.71	9.67	7.70	7.33	47.66	72.93	6.12	60.25	62.52
	Mean	0.49	0.92	0.54	0.62	0.13	0.43	0.49	0.12	0.45	0.50
	Std.-dev.	0.61	0.93	0.77	0.64	0.20	0.81	0.73	0.19	0.86	0.77
Sub sample 3	Min	0.02	0.01	0.02	0.00	0.00	0.00	0.00	0.00	0.00	0.00
	Max	4.07	8.82	11.23	14.84	7.26	48.60	63.21	6.38	44.93	67.15
	Mean	0.46	0.98	0.54	0.62	0.13	0.43	0.49	0.12	0.44	0.50
	Std.-dev.	0.49	0.81	0.74	0.79	0.20	0.81	0.73	0.19	0.85	0.78

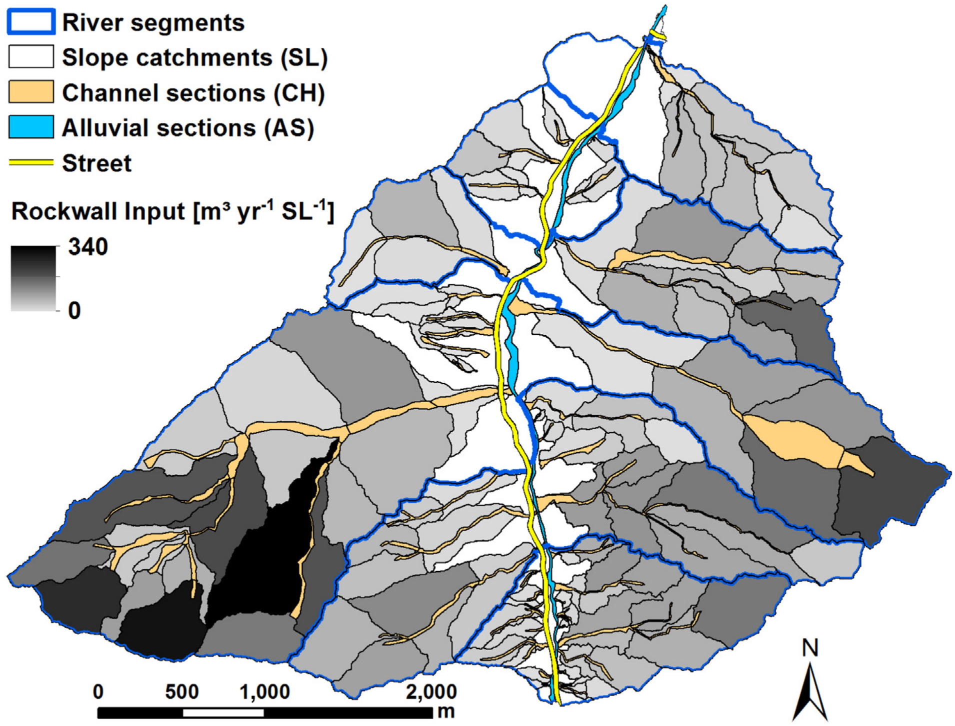

Fig. 6. Amount of sediment input through weathering processes from rock walls in the ZMS for each slope catchment.

affected channel section range from −17.8 to +5.2 m with a mean height change of −8.5 m. The adjacent slope catchments directly involved in the mining experienced elevation changes from −22.6 to +9.0 m, with a mean of −4.3 m. In the slope catchment closer to the outlet, elevation differences result from the preparation of the surrounding area to set up the former mining factory as well as the piling up of mined gravel (Fig. 2A bottom). In contrast, the slope catchment above talus cones (Fig. 2A top) reacts to the excavation of gravel at their footslopes. The remaining channel sections (range = −10.6 to +4.4 m, mean = −1.0 m) and slope catchments (range = −12.1 to +7.6 m, mean = −1.6 m) show, on average, rather small height differences besides some local extremes.

In the Langgries side catchment (Fig. 8A), sequences of erosion and deposition alternate along the channel sections. On average, processes of erosion/removal caused a mean elevation difference of −2.9 m (range = −7.9 to +3.0 m) in the lower parts. Channel sections farther upstream show a slight increase in elevation change (mean = +0.9 m) with peaks from −8.9 to +6.6 m at local extremes. Only those parts of the slope catchments bordering the channel sections are part of the observation area. Elevation changes in these areas range from −9.5 to +14.1 m with extreme values mainly recorded in the rear section of the Langgries catchment with a mean difference of +1.8 m.

4.2.2. Recent (2010–2015)

Areas of elevation differences (Fig. 9) are mostly (but not only) limited to channel and alluvial sections during the observation period from 2010 to 2015. Elevation differences in slope catchments occur at smaller spatial scales where small scale processes are reworking debris or rock fall accumulates. Only a few side catchments (e.g., Buckletschneider, Gseng, Kainzenalbl, Kaderalblschütt, Langgries) show changes of larger extent at some of their slope catchments. The mean height change throughout all slope catchments is −0.5 m, but differences occur focusing on the three segments of the ZMS. Deposition (mean = +0.6 m) prevails in segment III, whereas slope catchments belonging to segments II and I show erosion on average with mean height changes of −0.8 m and −0.7 m, respectively.

Elevation changes in channel sections have a larger spatial extent compared to slope catchments. Some of these channel systems inside a side catchment clearly show alternating patterns of erosion and deposition (e.g., Gseng, Kaderalblschütt, Langgries) over longer distances. Predominant erosion can be detected in channel sections mainly on the eastern side of segments I and III with direct access to the fluvial system. Channel sections on the western side (in segments I and III), mainly being barred by the road, show little change in elevation. Mean height changes throughout all channel sections add up to −0.1 m. On average, erosion and deposition seem to cancel each other out. Only channel sections at segment I clearly indicate an average loss in height (mean = −2.2 m), which is however largely influenced by the side catchment in the far north (Humlechner) where sediment has been removed anthropogenically during 2010–2011 (personal communication with NP Gesäuse). Focusing on the two most influential side catchments (Gseng, Fig. 7B and Langgries, Fig. 8B), with its channel sections being involved in the gravel mining show a vast area of accumulation. At Gseng these height changes range from −3.3 to +4.4 m (mean = +1.0 m) and are roughly limited to one channel section. The Langgries "conveyor belt" is continuously transporting sediment over a distance of nearly 1.5 km, showing alternating areas of erosion (down to −6.5 m) and deposition (up to +4.4 m), but eventually resulting in an average mean deposition of +0.2 m. In the final section (mainly affected by former mining), height changes range from −3.2 to +4.0 m with an average of +1.5 m.

The alluvial sections of the Johnsbach River are influenced by their neighboring sections and by the side catchments. The two segments III A and III B are characterized by erosion on average (III A: −0.2 m, III B: −0.5 m), with elevation differences ranging from −2.8 to +1.7 m and −7.5 to +1.7 m, respectively. Highest erosion values do usually occur at the edge of the alluvial sections where channel sections intersect with the fluvial system, whereas deposition can generally be detected on the opposite side of those confluences. The alluvial section of segment II B marks the only river reach where mean deposition (+0.4 m) can be assessed covering elevation differences in a range from −5.3 to +3.1 m. Typical fluvial patterns of erosion and deposition can be observed, which develop as the course of the river shifts

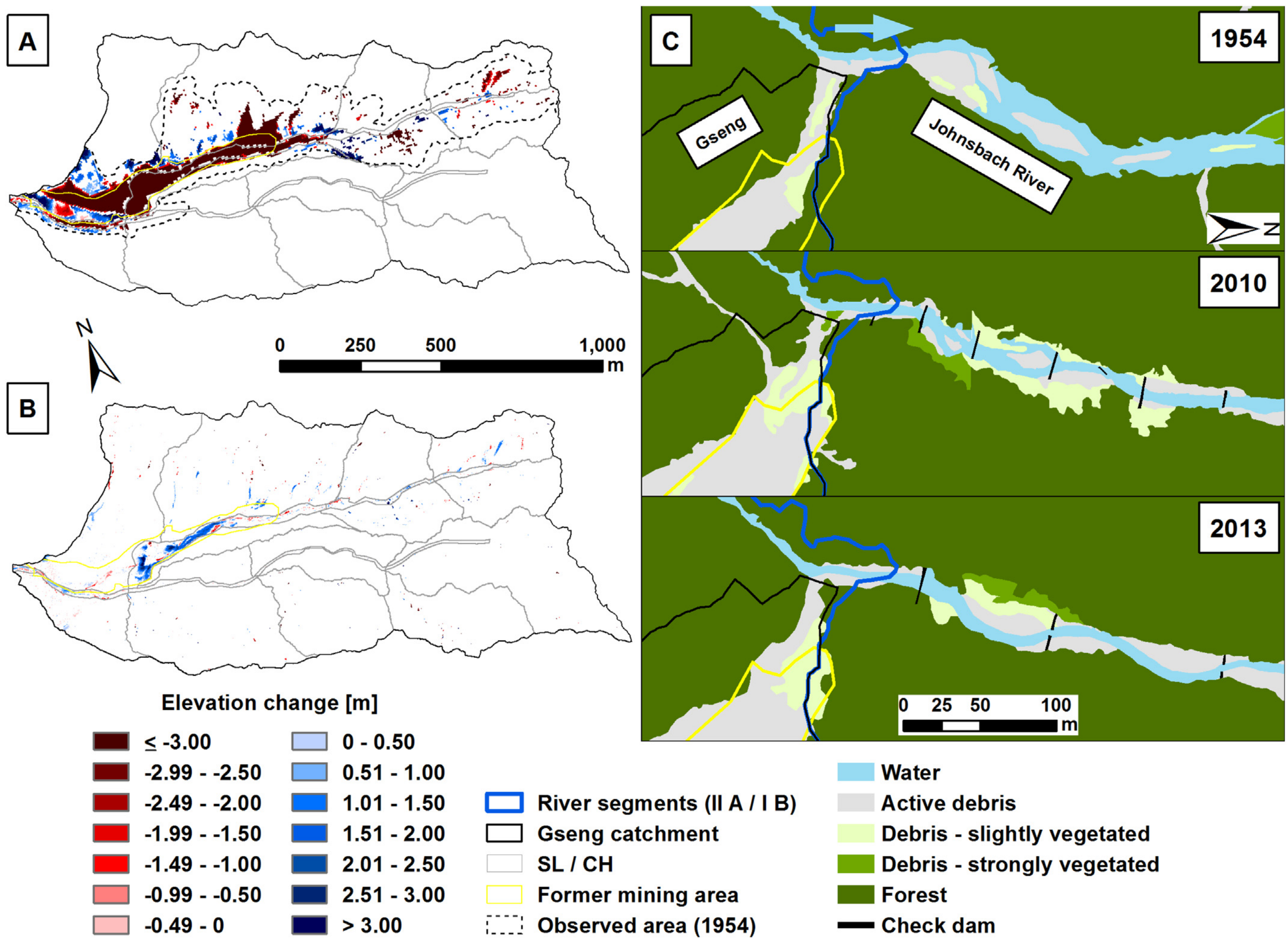

Fig. 7. (left) DoD maps of the Gseng side catchment: (A) 1954–2010; (B) 2010–2015. Colour scale ranges from red (erosion) to blue (deposition). DoD (1954–2010) was computed within a perimeter (dashed line) that includes areas featuring evidence of gravel mining and (resulting) geomorphic activity via photo interpretation and witness reports. (C) Maps of the Gseng outlet and the adjacent downstream river reach in 1954, 2010 and 2013 (for orientation see Fig. 9). Note: the blue arrow is indicating the direction of flow.

in its river bed. The next alluvial section in flow direction (II A) hardly shows any elevation change. The last two alluvial sections (river segments I A and I B) are similar in their behavior showing a meandering river course. Both sections are equivalent in terms of their mean elevation change (−0.3 m) and their local extremes (from −2.5 to +1.2 m).

4.3. Annual bedload transport

The bedload transport (of the fraction with grain sizes larger than 10 mm) at the Johnsbach River could be computed through the calibration of the geophones for the years 2016 and 2017. As an example, the average daily calculated bedload transport correlated well with measured daily mean water levels in the year 2016 (Fig. 10A). The annual bedload yield ($m^3\ yr^{-1}$) for the years 2016 and 2017 was derived by integrating the bedload transport over the time. The annual bedload yield of the years 2012 to 2015 could also be computed by correlating the water levels with the geophone data (Fig. 10B). The annual bedload yield of the grain fraction 1 mm to 10 mm was estimated on the basis of the medium particle size distribution from the slot sample measurements. Summing them up for the time period of 2012 to 2017, we determined an average bedload yield of about 6100 $m^3\ yr^{-1}$ at the Johnsbach River.

5. Discussion

5.1. Methodological progress – a new routing approach

Transported sediment volumes were routed along the cascading system chain (bedrock - slope catchment - channel section - alluvial section) in all side catchments and river segments. Sediment input was expected to occur due to rock fall events. Annual input rates were calculated using rock wall retreat rates for different rock types according to the geological setting. These sediment input volumes affect the net volume changes of the adjacent slope catchments (or channel sections and so on) derived from surface differencing. If net erosion prevails, sediment transport is routed farther through the system to the next compartment, for net deposition sediment transport is interrupted. Thus, a final sediment output volume is derived for each side catchment and river segment. As a result, it is possible to capture sediment dynamics from source to sink.

The novelty of the presented work lies in the combination of the sediment cascade investigation with the measurement of the bedload transport at the outlet of the catchment. Numerous qualitative geomorphometric approaches have addressed sediment connectivity (Cavalli et al., 2013) or the analysis of sediment routing (Stangl et al., 2016), but tend to miss the quantification of the sediment dynamics. With our novel routing approach, sediment is quantified and propagated

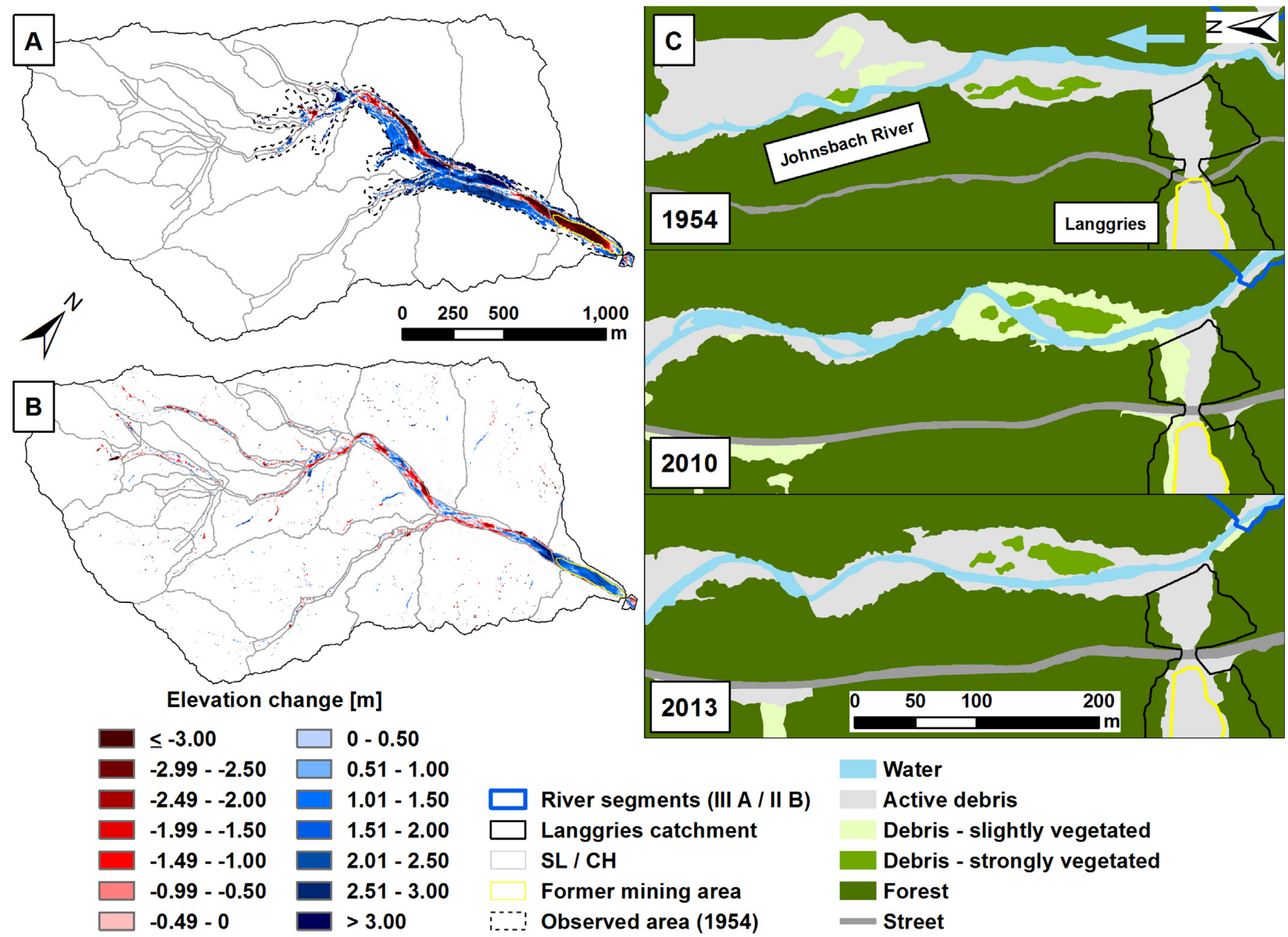

Fig. 8. (left) DoD maps of the Langgries side catchment: (A) 1954–2010; (B) 2010–2015. Colour scale ranges from red (erosion) to blue (deposition). DoD (1954–2010) was computed within a perimeter (dashed line) that includes areas featuring evidence of gravel mining and (resulting) geomorphic activity via photo interpretation and witness reports. (C) Maps of the Langgries outlet and the adjacent downstream river reach in 1954, 2010 and 2013 (for orientation see Fig. 9). Note: the blue arrow is indicating the direction of flow.

through the system and compared to actual measurements of bedload at the outlet. Furthermore, reconstruction of the former sediment cascade allows the evaluation of historical mining activities as well as their impact on recent sediment dynamics.

5.2. Sediment budget scenarios

Three sediment budget scenarios were developed (Fig. 11): (A) the period before 2010, representing the time of active gravel mining, (B) the time between 2010 and 2015, which reflects the current situation, and (C) a future scenario, assuming that the side catchments affected by mining will be finally coupled to their full extent.

5.2.1. Mining period (pre-2010)

During the time of active gravel mining (from 1984 and 1991, for Gseng and Langgries, respectively, to 2008) (Fig. 11A, Table 3) both side catchments were heavily affected. Calculated annual volumes that were excavated can be specified as 19,224 $m^3\ yr^{-1}$ at Gseng and 5672 $m^3\ yr^{-1}$ at Langgries (Table 4). The effects of gravel mining can be detected clearly in the DoD maps (Figs. 7A and 8A). The spatial extent of erosion/excavation corresponds very well with the outline of the former mining activities. Even though the DoD covers a longer period of time, the changes are still remarkable. In the southern part of ZMS (II B to III B), volumes of sediment input from the eastern side channels (in total 5870 $m^3\ yr^{-1}$) as well as net erosion inside the Johnsbach River (in total 900 $m^3\ yr^{-1}$) were assumed to be similar to the DoD of 2010–2015 since we have no observation for these reaches before 2010. The same is valid for sediment input into the ZMS from the catchment area above (~2500 $m^3\ yr^{-1}$), which is provided almost exclusively by a side catchment that is connected directly to the beginning of the ZMS. An estimation of volumetric change in the river reaches downstream of the Langgries side catchment (I A to II B) cannot be made. Since no sediment was delivered by Gseng and Langgries, the main channel has probably eroded the available sediment in the downstream direction leading to a narrowing of the active channel bed that can be seen in Figs. 7C and 8C. Accordingly, the final sediment output might be substantially larger than the estimated 10,350 $m^3\ yr^{-1}$.

5.2.2. Current situation (2010–2015)

At present (Fig. 11B), both side catchments experiencing former gravel show sediment output (with 630 $m^3\ yr^{-1}$ at each) that directly affects the river reaches downstream from those confluences. Especially downstream of Langgries the river section II B is characterized by area-wide deposition (Fig. 9) of 1490 $m^3\ yr^{-1}$. River reach I B, following the intersection with Gseng, shows a slightly different situation (Fig. 9 and Fig. 7C) as net erosion prevails at 390 $m^3\ yr^{-1}$. Still there are large amounts of sediment being deposited in the areas formerly influenced by excavation (Figs. 7B and 8B), which sum up to 1540 $m^3\ yr^{-1}$ at

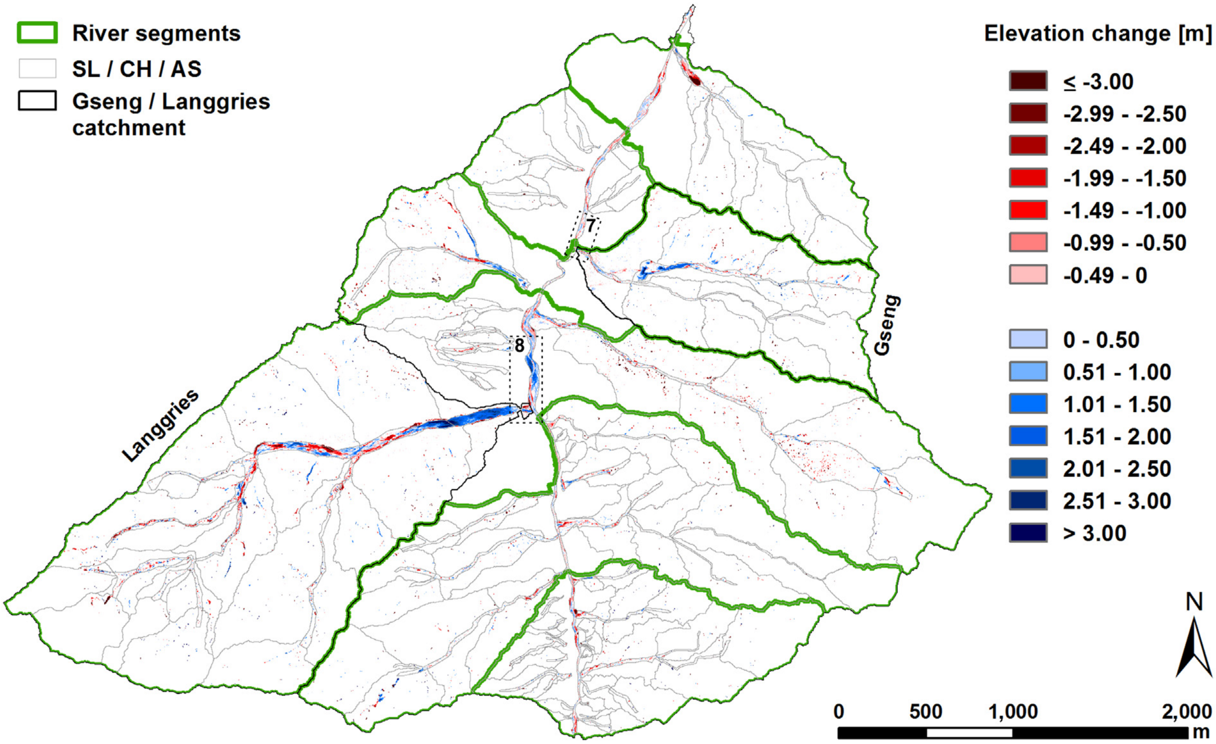

Fig. 9. DoD map of the ZMS (2010–2015). Colour scale ranges from red (erosion) to blue (deposition). Note: dashed rectangles indicate the positions of Figs. 7C and 8C.

Gseng and 6340 $m^3\ yr^{-1}$ at Langgries (Table 4). The southern half of ZMS, similar to pre-2010, shows high input from eastern side catchments and also from the area to the south entering the ZMS. On the western side of the Johnsbach River there are 1080 $m^3\ yr^{-1}$ potentially entering section III A from the side catchments Breitschütt, Mitterriegl and Buckletschneider. Due to medium-sized bridge openings it is not certain that the entire amount of sediment makes its way to the main river system. Farther downstream on the western side (sections I B and II A), undersized bridge openings completely block the sediment flow, which leads to deposition of sediment close to the street in orders of magnitude of around 2000 $m^3\ yr^{-1}$.

At both river reaches in section I (A and B), net erosion occurs with 370 $m^3\ yr^{-1}$ and 390 $m^3\ yr^{-1}$, respectively. In the northernmost side catchment (Humlechner) connected to river reach I A on the eastern side, 3780 $m^3\ yr^{-1}$ were eroded or removed from the area. This loss can be attributed to anthropogenic removal and is therefore not considered in the sediment budget. These observations lead to a current sediment yield of almost 11,000 $m^3\ yr^{-1}$ that is being delivered by the Johnsbach Valley to the River Enns. However, bedload monitoring occurring at the outlet of the ZMS reveals an annual bedload yield of 6100 $m^3\ yr^{-1}$. Explanations for the discrepancy of these two values can be found in Section 5.3.

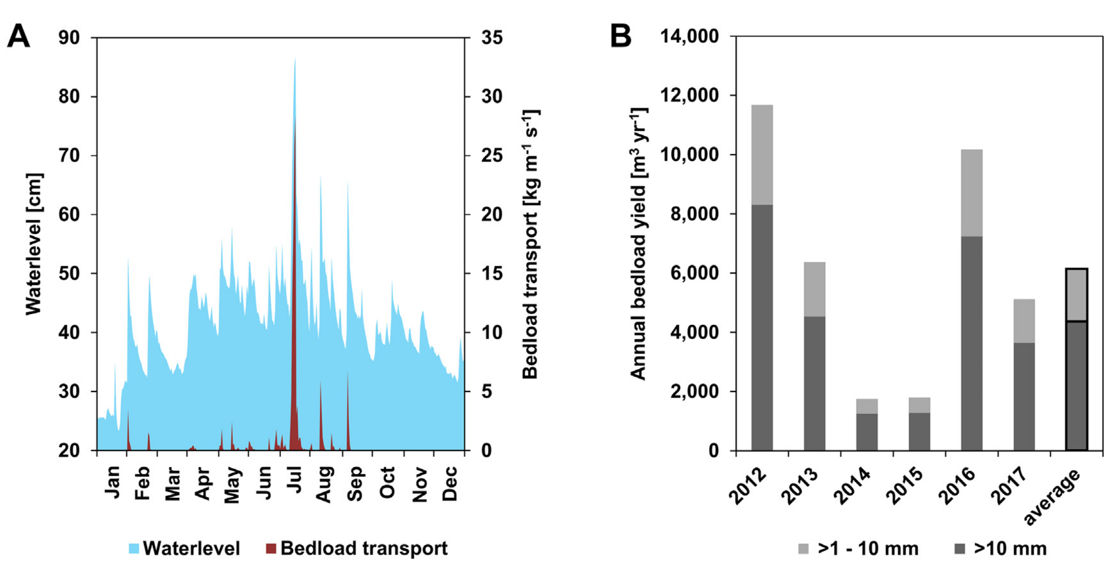

Fig. 10. (A) Water level (blue) and bedload transport (brown) of the Johnsbach River for the year 2016; (B) annual bedload yield at the outlet of the Johnsbach River for the years 2012 to 2017 for two grain size fractions.

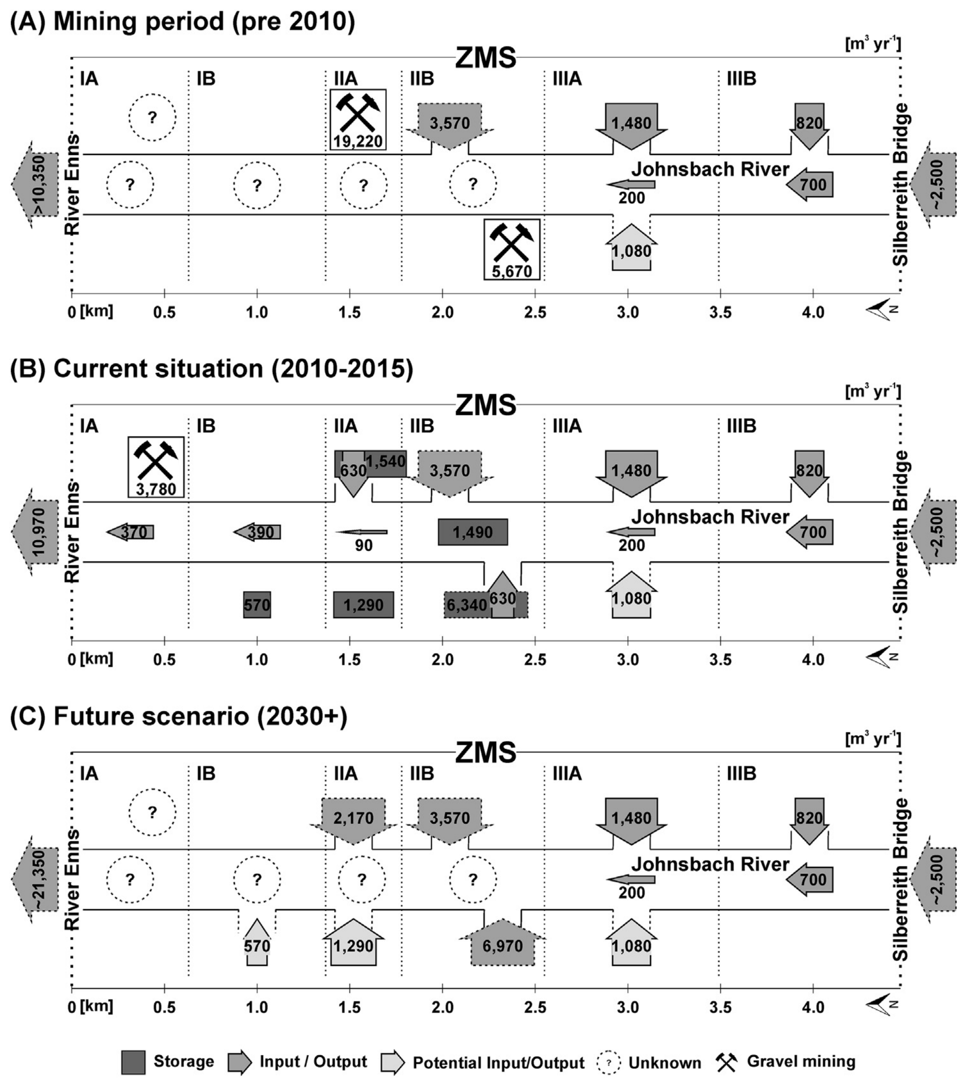

Fig. 11. Flow charts of annual sediment budget scenarios along the Johnsbach River between the Silberreith Bridge and the confluence with the River Enns (I A to III B refer to the river segments and reaches as defined in Section 2.2): (A) time of active gravel mining, (B) 2010–2015, (C) future scenario. Note: solid border of box or arrow is for true value/size ratio, dashed border is for untrue.

5.2.3. Future scenario (2030+)

In a future scenario (Fig. 11C) with an anthropogenically undisturbed sediment flow, much more sediment will be contributed by the side catchments to the main river system and potentially be washed out of the Johnsbach Valley. Once the side catchments with former gravel excavation (Gseng and Langgries) are fully connected, sediment output rates will rise to ~2200 $m^3\ yr^{-1}$ at Gseng and ~7000 $m^3\ yr^{-1}$ at Langgries. This will of course take some time since the mining history

Table 3
Volumetric rates of change (separated between slope catchments and channel sections, values are not propagated and represent the sum of each) and output at Gseng and Langgries side catchment only in the observed area of 1954 (see Figs. 7 and 8 for orientation). Note: time intervals marked (*) present the actual mining period with annual volumetric rates being calculated based on the period 1954–2010.

Side catchment	Erosion	Deposition	Erosion	Deposition	Output
	Slope catchments		Channel sections		
	[$m^3\ yr^{-1}$]				
Gseng					
1954–2010	5330	1014	3550	40	8737
2010–2015	1913	1922	663	2605	626
1984–2008*	12,438	2366	8284	93	19,224
Langgries					
1954–2010	222	3078	2175	1571	4622
2010–2015	5662	5218	8169	13,248	629
1991–2008*	733	10,140	7166	5176	5672

Table 4
Gravel excavation capacities and sediment delivery of the former mining areas in Gseng and Langgries. Note: *: propagated volume in the former mining areas.

	Gseng	Langgries
Mining area [m^2]	58,600	16,400
Mining period (1984/91–2008)		
Total excavated volume [m^3]	461,300	96,400
Years of excavation	24	17
Annual excavated volume (AEV) [$m^3\ yr^{-1}$]	19,220	5670
Excavation rate [$m^3\ m^{-2}\ yr^{-1}$]	0.33	0.35
Current situation (2010–2015)		
Total deposited volume [m^3]	7700	31,700
Years of observation	5	5
Annual deposited volume (ADV) [$m^3\ yr^{-1}$]*	1540	6340
Replenishment rate [$m^3\ m^{-2}\ yr^{-1}$]	0.03	0.39
Future scenario		
Recovery ratio (AEV/ADV)	12.5	0.9
Years to reach a balanced state	(300)	15

has caused enormous sinks that have to be refilled. Taking into account how much sediment has been excavated in the past and how fast the sediment bodies in both channel sections are now aggrading, this will take up to 300 yr at Gseng and about 15 yr at Langgries (Table 4). Besides that, several side catchments on the western side of the Johnsbach River (sections I B to III A) could contribute their output material (currently ~3000 m^3 yr^{-1}) to the main fluvial system if access would be enabled by means of wider bridge openings. As the sediment input volumes from the side catchments of the lower ZMS are changing, the adjacent river reaches will certainly react to a currently unknown degree and probably be transformed into a gravel-bed braided river system. Additionally, considering the sediment relocation from the southern half of the ZMS (assuming similar magnitudes as today), the total sediment output would likely increase to as much as 21,000 m^3 yr^{-1}.

5.3. Sources of uncertainty

Constructing a sediment budget is associated with several uncertainties that can arise from comparing measured to predicted amounts of sediment or by making assumptions for longer time periods than covered by the observations.

Since sediment input from rock wall retreat was calculated on the basis of reference values from the literature, there is the potential for uncertainty and spatial inhomogeneity in estimates of rock wall retreat. The latter point is not expected to change the budget significantly as local variations in sediment input are probably attenuated because of the integration in progressively larger units.

The current annual sediment yield at the outlet of the Johnsbach Valley can on the one hand be predicted to be almost 11,000 m^3 yr^{-1} (2010–2015) by the sediment budget model, and on the other hand be measured as ~6000 m^3 yr^{-1} (2012–2017) by the integrative bedload monitoring system. This deviation can result from the different observation periods.

The predicted amounts of excavated sediment at the formerly mined areas are derived from differencing DEMs over a long time period. These volumes are subject to qualitative uncertainties as there is no information available on sediment distributing processes or events during that time span for the study area.

Taking into account the actual area on which sediment was excavated, annual export rates are similar with 0.33 m^3 m^{-2} yr^{-1} and 0.35 m^3 m^{-2} yr^{-1} for Gseng and Langgries, respectively (Table 4). Since the mining activities ended, both side channels are reacting to the sediment supplied from upstream. Therefore, the main control on channel response and recovery appears to be the ratio between the former sediment extraction rate and the current replenishment rate (Rinaldi et al., 2005). During the observation period (2010–2015), sediment was deposited in the former mining areas with annual rates of 0.03 m^3 m^{-2} yr^{-1} and 0.39 m^3 m^{-2} yr^{-1} for Gseng and Langgries, respectively (Table 4). Assuming a constant rate of recharge, calculated recovery ratios (annual excavated volume divided by annual deposited volume) for Gseng (12.5) and Langgries (0.9) indicate that the time to reach a balanced state will be approximately 300 yr (Gseng) and 15 yr (Langgries), respectively. However, the current sediment transport direction at Gseng does not appear to follow the former channel as it goes around the area of the former mining factory (Fig. 7) to converge with the already existing channel (Fig. 2A). Thus, it can be assumed that a full connection to the fluvial system will be achieved much sooner than calculated.

5.4. Comparison to other catchment budgets

Kondolf (1994) described the procedure of sediment transport connecting zones of erosion and deposition in an idealized watershed using the term conveyor belt. Sediment is being moved in those zones of transport and added and subtracted from temporary storage sites in ways commonly not recognized. Similar findings were also reported by Calle et al. (2017), who observed channel changes in a Mediterranean river reach over a period of almost 70 yr following extensive instream gravel mining. They explained in detail the evolution at the interplay between gravel excavation and sediment recharge through floods. This trend can be observed in the Johnsbach Valley as well, especially in the Langgries area where sediment transport is now able to connect the sediment production zone to the outlet of the side catchment, thereby re-establishing sediment fluxes that cause significant changes in river reach morphology.

Other sediment budget studies in alpine areas have mainly focused on proglacial zones (e.g., Warburton, 1990) or worked on much longer timescales, preferably in closed settings without sediment export (Müller, 1999; Hinderer, 2001; Götz et al., 2013) and are, thus, not fully comparable to our approach. Rainato et al. (2017) derived their budget of the Rio Cordon catchment from a monitoring station at the outlet of the catchment only, without regarding sediment fluxes internal to the catchment. Similarly, Hinderer (2001) estimated modern denudation rates from river loads and delta surveys and published catchment-wide denudation rates of 30–360 mm ka^{-1}. Denudation rates for the Johnsbach catchment are well within the range of these values (168 mm ka^{-1} currently and up to 327 mm ka^{-1} in the future). However, taking into account that most of the exported sediment is supplied from the ZMS, as the sediment budget (Fig. 11) reflects, denudation rates for the ZMS aggregate to 843 mm ka^{-1} currently and 1641 mm ka^{-1} in the future, which confirms this is a highly morphodynamic system.

5.5. Morphological changes in mined areas

At Langgries, sediment was continuously excavated in the first 300–400 m upstream of the road (Fig. 8A) resulting in a topographic depression that is being refilled episodically since the end of the mining period. It appears that the over-steepened knickpoint at the upper end of the mining pit has eroded farther upstream since the total length of the depression is much longer than the actual mining area (Fig. 8B). The current sediment dynamics have been investigated by Rascher and Sass (2017) during a two year observation period showing that although sediment transport varies at different sections along the lower Langgries side channel, there is a clear tendency for refilling the mining gap. The Gseng catchment was affected rather differently by gravel excavation because the lower parts were prepared to set up a factory to process the gravel immediately. The actual sediment mining occurred about 500 m inside the side catchment. While excavating at the footslopes of the talus cones and sheets (Fig. 7A), retrograde erosion is causing the exhumation of the talus-covered bedrock by continuously refilling the actual working zone. This principle is described by Calle et al. (2017) as floods of different magnitudes reshape formerly mined areas by incising into the fresh sediment exposing cemented alluvium and bedrock. Currently, sediment relocation inside Gseng is limited to the main channel where a constant shift of erosion and deposition occurs (Rascher and Sass, 2017) developing a lobe-shaped sediment front that slowly reclaims the flat area of the former mining factory (Fig. 7B). Therefore, the current sediment output can only be attributed to the unaffected sub-channel (Fig. 2A) on the orographic left side of the catchment.

5.6. Impact on river morphology

Assuming that the condition in 1954 represents a near-natural situation (Figs. 7C and 8C top), river reaches downstream from the confluences of the Johnsbach River and either Gseng or Langgries show large alluvial plains with active debris and a partially braided river system. During the mining period sediment input from those two side catchments was lacking, resulting in incision of the main river into the available sediments and, subsequently, channel narrowing. Some parts inside the channel gained vegetation cover that stabilized the formerly active debris. This situation culminated around 2010 (Figs. 7C and 8C middle) when active mining was finally prohibited and river restoration measures were showing their impact. Subsequently, both river reaches show aggradation and channel widening again by refilling the missing sediment from the two side catchments (Figs. 7C and 8C bottom). These sequences of river degradation/aggradation and channel narrowing/widening are well known in this context of gravel mining and were already described by many authors in either perennial (e.g., Rinaldi et al., 2005; Rivora et al., 2005; Martín-Vide et al., 2010) or ephemeral river reaches (e.g., Sandecki and Avila, 1997; Downs et al., 2013; Calle et al., 2017) all around the world. For the future it is difficult to predict sediment dynamics, especially in the alluvial sections I A to II B, as this depends on the connectivity of the adjacent side catchments and the associated sediment input rates. On the one hand, sediment is stored adjacent to the road on the western side of the river, which could be made available if the coupling behavior of the corresponding suppling catchments improved. On the other hand, stored sediment was removed from the Humlechner catchment (Section I A) in 2011 because it posed a potential threat to the infrastructure downstream. Therefore, the natural sediment dynamics cannot be fully predicted.

5.7. Consequences for river ecology, natural hazards and hydropower

Intensified sediment transport inside the fluvial system was one of the main goals of the river restoration LIFE-project from 2006 to 2009. It will remain for future investigations to determine how this increased bedload will influence habitat creation and fish migration, as considered in the restoration plan; the first investigations by the NP Gesäuse are encouraging. Moreover, the increased sediment yield will widen the riverbed and thus, put the new reduced river training measures to a test. Furthermore, the additional sediments will considerably impact the mouth of the Johnsbach River into the River Enns and will be recognizable in the dam basin of the hydropower plant some kilometers downstream, causing higher maintenance costs. Sediment availability will not be a limiting factor in the Johnsbach Valley because the ZMS provides large amounts of sediment already, and most certainly if the full connection of the two formerly mined side catchments persists. However, it remains to be seen how the ZMS will continue to develop ecologically and in terms of extreme events and natural hazards as the entire system is still responding to the renaturation measures.

6. Conclusion

During the past 70 yr, anthropogenic action in the Johnsbach Valley has interfered with natural sediment dynamics. River engineering measures were installed to protect the local population and infrastructure from flood disasters. Gravel mining in two of the largest side channels was preventing sediment from being delivered to the main fluvial system. The resulting sediment deficiency in the Johnsbach River was one of the main causes leading to river restoration strategies and river management. In the present study sediment dynamics were investigated in the ZMS by use of a sediment budget to characterize the past, present and future sediment flows. The main results can be summarized as follows:

- During the mining period the annual amount of sediment retained was ~25,000 m^3 yr^{-1}, which resulted in a deficit of sediment available for refilling in the fluvial system. Nevertheless, with the sediment supply from the undisturbed side catchments in the ZMS (~9500 m^3 yr^{-1}) an annual sediment export can be adjusted to ~10,000 m^3 yr^{-1}.
- Currently sediment is refilling the sinks resulting from gravel excavation in the Gseng and Langgries side catchments at a rate of ~8000 m^3 yr^{-1}. Furthermore, both side channels are again connected to the fluvial system (~1200 m^3 yr^{-1}), though not yet to its full extent. Adjacent river reaches are now responding differently to this changed sediment transport behavior leading to a final sediment export of ~11,000 m^3 yr^{-1}.
- If in the near future all side channels are coupled to the full extent, increased sediment availability will probably cause sediment relocations and supply to the fluvial system at higher rates. Therefore, sediment transport within the Johnsbach River will increase and could lead to a doubling of the annual sediment output compared to the current situation.
- In addition to the positive effects of increased sediment availability on river restoration, a higher sediment flux could also be evaluated as critical. River managers in the future must be aware of an increased sediment supply to the nearby road as well as to the hydroelectric power plant at the River Enns downstream. Higher costs for maintenance at both would then have to be expected.

Acknowledgements

The authors would like to thank the Bureau of the Styrian Government for compiling and providing the DEM database of 2010. We also thank the NP Gesäuse for making data on water level gauging and vegetation cover, resulting from HABITALP (Alpine Habitat Diversity) mapping, available to us. Funding was provided by the Austrian Science Fund (FWF, P24759) in the context of the Sedyn-X project and the Austrian Service of Torrent and Avalanche Control at the Austrian Federal Ministry of Agriculture, Forestry, Environment and Water Management. Furthermore, we would express our great thanks to several colleagues and students (Johann Aigner, Nicole Kamp, Paul Krenn, Jana Obermeier, Matthias Rode, Harald Schnepfleitner, Johannes Stangl) who helped in obtaining and preparing data during field campaigns or in the office. Scott A. Lecce and two anonymous referees contributed to this paper by providing useful remarks, comments and suggestions, which is gratefully acknowledged.

Appendix A

Table A.1
Alluvial sections with specific parameters and volumetric rates (2010–2015) of sediment input (from the reach above as well as from the adjacent side catchments), storage change and sediment output (to the reach below and at the outlet of the catchment, respectively).

Alluvial Sections	Area		Elevation		Slope	Input	Erosion	Deposition	Output
	[m^2]		[m a.s.l.]		[°]	[m^3]			
	Plan	Surface	Min	Max	Mean	Annual			
I A	16,689	17,186	585	591	10	9532	580	209	9903
I B	18,048	18,778	601	628	13	9145	603	216	9532
II A	6057	6782	618	636	27	9051	117	28	9141
II B	29,737	30,839	631	660	12	9917	892	2383	8425
III A	13,279	14,018	652	678	15	5517	306	103	5719
III B	16,008	16,932	676	723	16	3331	965	262	4033

Table A.2
Side catchments (grouped into alluvial sections) with specific parameters and volumetric rates (2010–2015) of sediment input (sum of all slope catchments as defined in Fig. 6), storage change (divided between slope catchments and channel sections, values are not propagated and represent the sum of each) and sediment output.

#	Side catchments	Area		Elevation		Slope	Bedrock[a]	Vegetation[b]	Input	Erosion	Deposition	Erosion	Deposition	Output	Riverside	Connection[c]
										slope catchments		channel sections				
		[m²]		[m a.s.l.]		[°]	[%]	[%]	[m³]							
		plan	surface	min	max	mean	total	mean	annual							
	I A															
1	Humlechner	704,130	1,183,195	590	1336	60	49	66	248	1247	1079	3231	125	3778	Right	Excavation
	I B															
2	Unnamed XI	13,990	36,881	603	932	76	65	25	7	1	7	0	2	0	Right	River
3	Amtmanngalgen	22,855	33,399	607	868	53	17	79	2	9	26	6	33	0	Left	Street
4	Neuweg	162,495	253,374	610	1027	53	45	59	56	110	105	181	18	234	Left	Street
5	Unnamed XII	48,548	76,701	613	931	56	45	75	7	28	29	4	4	4	Right	River
6	Unnamed X	63,745	97,951	617	974	55	23	90	3	263	76	157	17	332	Left	Street
	II A															
7	Gseng	1,137,886	2,010,926	619	1623	67	58	40	809	2340	2251	676	2652	626	Right	River
8	Kaderalblschütt	509,849	710,646	638	1197	51	20	69	84	2590	1114	539	827	1293	Left	Street
	II B															
9	Kainzenalbl	1,511,767	2,820,887	636	2334	74	58	48	673	3394	1569	2165	795	3569	Right	River
10	Unnamed XIV	131,026	183,491	642	1189	49	12	89	5	289	68	9	5	231	Left	Street
11	Langgriesrunse II	32,391	53,671	648	999	64	30	74	4	178	336	12	96	0	Left	Street
12	Langgriesrunse I	25,701	39,370	649	1000	60	50	69	6	17	8	172	79	109	Left	Street
13	Unnamed XV	23,022	31,235	662	1010	45	27	77	4	58	2	9	28	41	Left	Forest
14	Unnamed XVI	7694	10,690	680	842	45	24	64	2	0	0	10	9	3	Left	Forest
15	Langgries	3,302,159	6,011,413	652	2251	71	56	44	2352	7646	6506	8847	14,016	629	Left	River
	III A															
16	Petergstammplan II	262,325	441,216	655	1346	61	57	66	100	493	235	228	42	544	Right	River
17	Unnamed I	2713	6074	657	762	69	67	24	3	1	5	0	1	0	Right	River
18	Unnamed III	13,318	23,790	659	825	61	82	25	14	1	1	12	3	23	Right	River
19	Petergstammplan I	81,208	140,928	663	1075	65	38	36	44	103	81	334	226	175	Right	Forest
20	Breitschütt	118,035	177,898	664	1178	54	28	69	36	421	110	69	79	337	Left	Street/River[d]
21	Petergstamm	818,222	1,640,497	669	2164	70	78	41	706	573	824	639	286	916	Right	River
22	Mitterriegel	294,617	488,937	671	1431	61	54	59	149	309	246	203	239	199	Left	Street/River[d]
23	Buckletschneider	661,448	1,200,644	676	1564	68	73	49	445	1221	1710	447	320	539	Left	Street/River[d]
	III B															
24	Bucklet opposite	44,753	134,673	677	1140	79	70	17	87	56	93	83	294	11	Right	River
25	Unnamed XVII	8593	13,860	683	903	55	23	85	1	9	31	2	8	0	Left	Street
26	Unnamed V	158,426	449,195	686	1359	78	81	19	268	198	590	193	289	178	Right	River
27	Unnamed XVIII	12,869	22,149	687	906	63	42	67	6	1	39	1	29	0	Left	Street
28	Unnamed XIII	7079	16,137	686	823	75	49	79	4	2	10	0	1	0	Right	River
29	Unnamed IV	7633	11,324	689	930	49	74	86	1	0	0	1	3	0	Left	Street
30	Fehringerkreuz III	46,740	87,132	692	1135	65	73	54	21	31	16	30	86	0	Left	Street
31	Unnamed VI	8826	20,666	689	855	73	70	21	13	11	2	32	8	46	Right	River
32	Unnamed VIII	1350	2951	689	798	72	48	11	2	0	0	0	2	0	Right	River
33	Fehringerkreuz II	26,578	47,931	694	1056	63	83	59	17	4	22	8	14	0	Left	Street
34	Unnamed VII	2214	4517	690	796	72	51	37	2	0	2	0	1	0	Right	River
35	Fehringerkreuz I	60,426	120,177	699	1174	73	78	49	39	58	30	69	68	68	Left	Street
36	Roteneder	483,155	1,077,723	695	1818	74	83	39	480	454	922	348	120	500	Right	River
37	Unnamed IX	100,787	204,295	696	1222	69	85	40	86	132	263	30	53	66	Right	River
38	Straussenalbl I	8311	17,577	700	890	67	85	51	6	3	6	25	6	22	Right	River
39	Unnamed II	17,137	37,014	706	946	74	70	69	2	5	16	1	0	2	Left	River
40	Straussenalbl II	3897	7079	710	954	61	78	39	1	0	1	7	5	1	Right	Street
41	Straussenalbl III	27,924	63,984	708	1078	77	69	38	9	19	57	13	17	0	Right	River

[a] In percent of total area.
[b] Mean degree of vegetation cover.
[c] Defines the sink of sediment output.
[d] Uncertain due to undersized bridge openings.

References

Ampferer, O., 1935. Geologischer Führer für die Gesäuseberge. Mit einer geol. Karte i. M. 1:25,000, Kartenerläuterungen und Beschreibung von 16 Wanderungen. Geologische Bundesanstalt, Wien (in German).

Brasington, J., Langham, J., Rumsby, B., 2003. Methodological sensitivity of morphometric estimates of coarse fluvial sediment transport. Geomorphology 53, 299–316.

Bravard, J.P., Amoros, C., Pautou, G., Bornette, G., Bournaud, M., Creuzé Des Chatelliers, M., Gilbert, J., Peiry, J., Perrin, J., Tachet, H., 1997. River incision in south-east France: morphological phenomena and ecological effects. Regul. Rivers Res. Manag. 13, 75–90.

Bravard, J.P., Kondolf, G.M., Piégay, H., 1999. Environmental and societal effects of river incision and remedial strategies. In: Simon, A., Darby, S.E. (Eds.), Incised River Channels: Processes, Forms, Engineering, and Management. John Wiley, Chichester, pp. 303–341.

Bunte, K., Abt, S.R., Potyondy, J.P., Ryan, S.E., 2004. Measurement of coarse gravel and cobble transport using portable bedload traps. J. Hydraul. Eng. 130, 879–893.

Calle, M., Alho, P., Benito, G., 2017. Channel dynamics and geomorphic resilience in an ephemeral Mediterranean river affected by gravel mining. Geomorphology 285, 333–346.

Cavalli, M., Trevisani, S., Comiti, F., Marchi, L., 2013. Geomorphometric assessment of spatial sediment connectivity in small Alpine catchments. Geomorphology 188, 31–41.

Downs, P.W., Dusterhoff, S.R., Sears, W.A., 2013. Reach-scale channel sensitivity to multiple human activities and natural events: lower Santa Clara River, California, USA. Geomorphology 189, 121–134.

Fischlschweiger, M., 2004. Untersuchung der Auswirkungen der Einstellung des Schotterabbaues im Unterlauf des Langriesgrabens. (Diploma Thesis). Höheren Bundeslehranstalt für Forstwirtschaft Bruck an der Mur, Austria (in German).
Flügel, H.W., Neubauer, F., 1984. Steiermark – Geologie der Österreichischen Bundesländer in kurzgefassten Einzeldarstellungen. Geologische Bundesanstalt, Wien (in German).
Fuller, I.C., Large, A.R.G., Charlton, M.E., Heritage, G.L., Milan, D.J., 2003. Reach-scale sediment transfers: an evaluation of two morphological budgeting approaches. Earth Surf. Process. Landf. 28, 889–903.
Glade, T., 2005. Linking debris-flow hazard assessments with geomorphology. Geomorphology 66, 189–213.
Götz, J., Otto, J.-C., Schrott, L., 2013. Postglacial sediment storage and rockwall retreat in a semi-closed inner-alpine sedimentary basin (Gradenmoos, Hohe Tauern, Austria). Geogr. Fis. Din. Quat. 36, 63–80.
Habersack, H., Piégay, H., 2008. River restoration in the Alps and their surroundings: past experience and future challenges. In: Habersack, H., Piégay, H., Rinaldi, M. (Eds.), Gravel-bed Rivers VI - From Process Understanding to River Restoration. Elsevier, Amsterdam, pp. 703–738.
Habersack, H., Kreisler, A., Rindler, R., Aigner, J., Seitz, H., Liedermann, M., Laronne, J.B., 2017. Integrated automatic and continuous bedload monitoring in gravel bed rivers. Geomorphology 291, 80–93.
Haseke, H., 2006. A2 Managementplan, Revitalisierungsprojekt Johnsbach-Zwischenmäuer 2006-2008. LIFE Report of the NP Gesäuse GmbH, Weng im Gesäuse, Austria (in German).
Haseke, H., 2011. Final Report - Abschlussbericht. LIFE Report of the NP Gesäuse GmbH. Weng im Gesäuse, Austria (in German).
Hiessleitner, G., 1935. Zur Geologie der Erz führenden Grauwackenzone des Johnsbachtales. Jahrb. Geol. Bundesanst. 85, 81–102 (in German).
Hinderer, M., 2001. Late quaternary denudation of the Alps, valley and lake fillings and modern river loads. Geodin. Acta 14, 231–263.
Holzinger, A., Haseke, H., Stocker, E., 2012. Managementplan - Witterschutt und Geschiebe. LIFE Report of the NP Gesäuse GmbH. Weng im Gesäuse, Austria (in German).
Kammerer, H., 2006a. Biotopkartierung Gesäuse - Teilbericht Kartierungsbereich Langgries. Survey on Behalf of NP Gesäuse GmbH, Weng im Gesäuse, Austria (in German).
Kammerer, H., 2006b. Biotopkartierung Gesäuse - Teilbericht Kartierungsbereich Gseng. Survey on Behalf of NP Gesäuse GmbH, Weng im Gesäuse, Austria (in German).
Kammerer, H., 2008. Biotopkartierung Gesäuse - Teilbericht Kartierungsbereich Johnsbach inkl. Humlechnergraben. Survey on Behalf of NP Gesäuse GmbH, Weng im Gesäuse, Austria (in German).
Kondolf, G.M., 1994. Geomorphic and environmental effects of instream gravel mining. Landsc. Urban Plan. 28, 225–243.
Kreisler, A., Moser, M., Aigner, J., Rindler, R., Tritthart, M., Habersack, H., 2017. Analysis and classification of bedload transport events with variable process characteristics. Geomorphology 291, 57–68.
Krenn, P., 2016. Kartierung und Evaluierung von Sedimenttransport-Prozessen in der Zwischenmäuerstrecke, Johnsbachtal. (Master Thesis). University of Graz, Austria (in German).
Lane, S.N., Westaway, R.M., Hicks, D.M., 2003. Estimation of erosion and deposition volumes in a large, gravel-bed, braided river using synoptic remote sensing. Earth Surf. Process. Landf. 28, 249–271.
Lieb, G.K., Premm, M., 2008. Das Johnsbachtal – Werdegang und Dynamik im Formenbild eines zweigeteilten Tales. In: NP Gesäuse GmbH (Ed.), Der Johnsbach. Schriften des NP Gesäuse 3, Weng im Gesäuse, pp. 12–24 (in German).
Liébault, F., Piégay, H., 2001. Assessment of channel changes due to long-term bedload supply decrease, Roubion River, France. Geomorphology 36, 167–186.
Liébault, F., Piégay, H., 2002. Causes of 20th century channel narrowing in mountain and piedmont rivers of southeastern France. Earth Surf. Process. Landf. 27, 425–444.
Liébault, F., Gomez, B., Page, M., Marden, M., Peacock, D., Richard, D., Trotter, C.M., 2005. Land-use change, sediment production and channel response in upland regions. River Res. Appl. 21, 739–756.
Liébault, F., Piégay, H., Frey, P., Landon, N., 2008. Tributaries and the management of main-stem geomorphology. In: Rice, S., Roy, A., Rhoads, B.L. (Eds.), River Confluences and the Fluvial Network. John Wiley, Chichester, pp. 243–270.
Marston, R.A., Girel, J., Pautou, G., Piégay, H., Bravard, J.P., Arneson, C., 1995. Channel metamorphosis, floodplain disturbance and vegetation development: Ain River, France. Geomorphology 13, 121–131.
Martinet, F., Dubost, M., 1992. Die letzten naturnahen Alpenflüsse. vol. 11. S kleine Schriften, chriften, Internationale Alpenschutzkommission CIPRA, Vaduz, Liechtenstein (in German).
Martín-Vide, J.P., Ferrer-Boix, C., Ollero, A., 2010. Incision due to gravel mining: modeling a case study from the Gállego River, Spain. Geomorphology 117 (3–4), 261–271.
Mühlhofer, L., 1933. Schwebstoff- und Geschiebemessungen am Inn bei Kirchbichl (Tirol). Wasserwirtsch. Wassertech. 28 (4), 37–41 (in German).
Müller, B.U., 1999. Paraglacial sedimentation and denudation processes in an Alpine valley of Switzerland. An approach to the quantification of sediment budget. Geodin. Acta 12 (5), 291–301.
Petts, G.E., 1989. Historical analysis of fluvial hydrosystems. In: Petts, G.E. (Ed.), Historical Change of Large Alluvial Rivers, Western Europe. John Wiley, Chichester, pp. 1–18.
Piégay, H., Darby, S.E., Mosselman, E., Surian, N., 2005. A review of techniques available for delimiting the erodible river corridor: a sustainable approach to managing bank erosion. River Res. Appl. 21, 773–789.
Rainato, R., Mao, L., García-Rama, A., Picco, L., Cesca, M., Vianello, A., Preciso, E., Scussel, G.R., Lenzi, M.A., 2017. Three decades of monitoring in the Rio Cordon instrumented basin: sediment budget and temporal trend of sediment yield. Geomorpholgy 291, 45–56.
Rascher, E., Sass, O., 2017. Evaluating sediment dynamics in tributary trenches in an alpine catchment (Johnsbachtal, Austria) using multi-temporal terrestrial laser scanning. Z. Geomorphol. 61 (Supplement 1), 27–52.
Rickenmann, D., Fritschi, B., 2017. Bedload transport measurements with impact plate geophones in two Austrian mountain streams (Fischbach and Ruetz): system calibration, grain size estimation, and environmental signal pick-up. Earth Surf. Dyn. 5 (4), 669–687.
Rickenmann, D., McArdell, B.W., 2007. Continuous measurement of sediment transport in the Erlenbach stream using piezoelectric bedload impact sensors. Earth Surf. Process. Landf. 32, 1362–1378.
Rickenmann, D., Turowski, J.M., Fritschi, B., Wyss, C., Laronne, J., Barzilai, R., Reid, I., Kreisler, A., Aigner, J., Seitz, H., Habersack, H., 2014. Bedload transport measurements with impact plate geophones: comparison of sensor calibration in different gravel-bed streams. Earth Surf. Process. Landf. 39, 928–942.
Rinaldi, M., Wyzga, B., Surian, N., 2005. Sediment mining in alluvial channels: physical effects and management perspectives. River Res. Appl. 21, 805–828.
Rinaldi, M., Simoncini, C., Piégay, H., 2009. Scientific strategy design for promoting a sustainable sediment management: the case of the Magra River (Central - Northern Italy). River Res. Appl. 25, 607–625.
Rivora, A., Batalla, R.J., Sala, M., 2005. Response of a river sediment budget after historical gravel mining (The Lower Tordera, NE Spain). River Res. Appl. 21, 829–847.
Sandecki, M., 1989. Aggregate mining in river systems. Calif. Geol. 42, 88–93.
Sandecki, M., Avila, C.C., 1997. Channel adjustments front instream mining: San Luis Rey River, San Diego County, California. Rev. Eng. Geol. 11, 39–48.
Sass, O., 2005. Spatial patterns of rockfall intensity in the northern Alps. Z. Geomorphol. Supplement 138, 51–65.
Sass, O., 2007. Bedrock detection and talus thickness assessment in the European Alps using geophysical methods. J. Appl. Geophys. 62, 254–269.
Sass, O., Wollny, K., 2001. Investigations regarding Alpine talus slopes using ground-penetrating radar (GPR) in the Bavarian Alps, Germany. Earth Surf. Process. Landf. 26, 1071–1086.
Spink, A., Fryirs, K., Brierley, G., 2009. The relationship between geomorphic river adjustment and management actions over the last 50 years in the upper Hunter Catchment, NSW, Australia. River Res. Appl. 25, 904–928.
Stangl, J., Rascher, E., Sass, O., 2016. Comparative analysis of sediment routing in two different alpine catchments. In: Beylich, A.A., Dixon, J.C., Zwolinski, Z. (Eds.), Source-to-sink-fluxes in undisturbed cold environments. Cambridge University Press, Cambridge, pp. 364–377.
Strasser, U., Marke, T., Sass, O., Birk, S., 2013. John's creek valley: a mountainous catchment for long-term interdisciplinary human-environment system research in Upper Styria (Austria). Environ. Earth Sci. 69, 695–705.
Surian, N., Rinaldi, M., 2003. Morphological response to river engineering and management in alluvial channels in Italy. Geomorphology 50 (4), 307–326.
Surian, N., Rinaldi, M., Pellegrini, L., Audisio, C., Maraga, F., Teruggi, L., Turitto, O., Ziliani, L., 2009a. Channel adjustments in northern and central Italy over the last 200 years. In: James, L.A., Rathburn, S.L., Whittecar, G.R. (Eds.), Management and Restoration of Fluvial Systems with Broad Historical Changes and Human Impacts. Geological Society of America Special Paper 451, Boulder, CO, pp. 83–95.
Surian, N., Ziliani, F., Comiti, F., Lenzi, M.A., Mao, L., 2009b. Channel adjustments and alteration of sediment fluxes in gravel-bed rivers of North-Eastern Italy: potentials and limitations for channel recovery. River Res. Appl. 25, 551–567.
Taylor, J., 1997. An Introduction to Error Analysis: The Study of Uncertainties in Physical Measurements. University Science Books, Sausalito, CA.
Thonhauser, H.C., 2007. Gewässerstruktur und Verbauungsgeschichte im Einzugsgebiet des Johnsbaches. (Diploma Thesis). University of Graz, Austria (in German).
Van Rijn, L., 1986. Manual Sediment Transport Measurements. Delft Hydraulics Laboratory, Netherlands.
Vehling, L., 2016. Gravitative Massenbewegungen an alpinen Felshängen: Quantitative Bedeutung in der Sedimentkaskade proglazialer Geosysteme (Kaunertal, Tirol). (PhD Thesis). University of Erlangen-Nürnberg, Germany (in German).
Vericat, D., Wheaton, J.M., Brasington, J., 2017. Revisiting the morphological approach: opportunities and challenges with repeat high-resolution topography. In: Tsutsumi, D., Laronne, B. (Eds.), Gravel-bed Rivers: Processes and Disasters. John Wiley, Chichester, pp. 121–158.
Wakonigg, H., 2012a. Klimaatlas Steiermark - Kapitel 2 - Temperatur. Zentralanstalt für Meteorologie und Geodynamik, Wien, Austria (in German).
Wakonigg, H., 2012b. Klimaatlas Steiermark - Kapitel 4 - Niederschlag. Zentralanstalt für Meteorologie und Geodynamik, Wien, Austria (in German).
Warburton, J., 1990. An alpine proglacial fluvial sediment budget. Geogr. Ann. Ser. A 72 (3/4), 261–272.

Ward, J.V., Tockner, K., Edwards, P.J., Kollmann, J., Bretschko, G., Gurnell, A.M., Petts, G.E., Rossaro, B., 1999. A reference river system for the alps: the 'Fiume Tagliamento'. Regul. Rivers Res. Manag. 15, 63–75.
Wheaton, J.M., 2008. Uncertainty in Morphological Sediment Budgeting of Rivers. (PhD Thesis). University of Southampton, England.
Wheaton, J.M., Brasington, J., Darby, S.E., Sear, D.A., 2010. Accounting for uncertainty in DEMs from repeat topographic surveys: improved sediment budgets. Earth Surf. Process. Landf. 35, 136–156.
Wyss, C., Rickenmann, D., Fritschi, B., Turowski, J.M., Weitbrecht, V., Boes, R., 2016. Measuring bed load transport rates by grain-size fraction using the Swiss plate geophone signal at the Erlenbach. J. Hydraul. Eng. 142 (5), 04016003.
Zulka, K.P., 2013. Analyse des Einflusses von Schotterbaggerungen auf die epigäische Arthropodenfauna im NP Gesäuse. Survey on behalf of NP Gesäuse GmbH, Weng im Gesäuse, Austria (in German).